DESIGN OF ARRAY ANTENNA FOR BODY CENTRIC COMMUNICATION

RAJESHREE A/P VEJASEGARAN

RESEARCH REPORT SUBMITTED IN PARTIAL FULFILMENT
OF THE REQUIREMENTS FOR THE DEGREE
OF MASTER OF ENGINEERING
(TELECOMMUNICATIONS)

FACULTY OF ENGINEERING
UNIVERSITY OF MALAYA
KUALA LUMPUR

2017

<div align="center">

UNIVERSITY OF MALAYA
ORIGINAL LITERARY WORK DECLARATION

</div>

Name of Candidate: V.RAJESHREE   (I.C/Passport No:

Matric No: KGE 150008

Name of Degree: MASTER OF ENGINEERING (TELECOMMUNICATIONS)

Title of Thesis: DESIGN OF ARRAY ANTENNA FOR BODY CENTRIC

COMMUNICATION

Field of Study: ANTENNA AND PROPAGATION

I do solemnly and sincerely declare that:

(1)   I am the sole author/writer of this Work;
(2)   This Work is original;
(3)   Any use of any work in which copyright exists was done by way of fair dealing and for permitted purposes and any excerpt or extract from, or reference to or reproduction of any copyright work has been disclosed expressly and sufficiently and the title of the Work and its authorship have been acknowledged in this Work;
(4)   I do not have any actual knowledge nor do I ought reasonably to know that the making of this work constitutes an infringement of any copyright work;
(5)   I hereby assign all and every rights in the copyright to this Work to the University of Malaya ("UM"), who henceforth shall be owner of the copyright in this Work and that any reproduction or use in any form or by any means whatsoever is prohibited without the written consent of UM having been first had and obtained;
(6)   I am fully aware that if in the course of making this Work I have infringed any copyright whether intentionally or otherwise, I may be subject to legal action or any other action as may be determined by UM.

Candidate's Signature   Date:

Subscribed and solemnly declared before,

Witness's Signature   Date:

Name:

Designation:

ii

ABSTRACT

The main aim of this research is to design single and multi-elements on-body antennas that operate at 2.4 GHz ISM band. The patch and the ground plane are designed using highly conductive pure copper while three dielectric materials are used as the substrate for comparison purposes. The antenna design are simulated using CST Microwave Studio. Several characteristics of the antenna such as reflection coefficient, bandwidth, VSWR, efficiency and radiation pattern are evaluated for both free space and on-body application. The comparison results reveal that the antennas design using RT Duroid 5880 result in low gain loss. Only small difference in reflection coefficient, S_{11} and bandwidth is observed for the array antennas as a consequence of variation in body tissue thickness. The increase in the fat layer thickness also resulted in a steady increase in gain for all antenna configurations. In order to minimize the attenuation of antenna performance in close proximity with the human body, simple gain improvement techniques are utilized. Antenna simulated gain is improved by 7.2 % for the first design and 8.4 % for the second design of 2x1 array antenna and 4.7 % for 4x1 array antenna.

ABSTRAK

Tujuan utama penyelidikan ini adalah untuk mereka bentuk antena tunggal dan berbilang elemen yang diletakkan di atas badan beroperasi pada 2.4 GHz. *Patch* dan *ground plane* direka dengan menggunakan tembaga tulen yang sangat konduktif manakala tiga bahan dielektrik digunakan sebagai substrat untuk tujuan perbandingan. Simulasi reka bentuk yang dihasilkan adalah menggunakan Microwave CST Studio. Beberapa ciri antena seperti pekali pantulan, jalur lebar, VSWR, kecekapan dan corak radiasi dinilai untuk ruang bebas dan aplikasi di atas badan. Hasil perbandingan menunjukkan bahawa reka bentuk antena yang menggunakan RT Duroid 5880 menyebabkan kehilangan kuas yang rendah. Hanya perbezaan kecil dalam koefisien pantulan, S_{11} dan jalur lebar diperhatikan untuk *antena array* akibat variasi dalam ketebalan tisu badan. Peningkatan ketebalan lapisan lemak juga mengakibatkan peningkatan kuasa dalam semua konfigurasi antenna. Untuk mengurangkan penguragan prestasi antena dekat dengan tubuh manusia, teknik penambahbaikan kuasa dilaksanakan. Kuasa antena diperbaiki sebanyak 7.2% untuk reka bentuk pertama dan 8.4% untuk reka bentuk kedua *antena array 2x1* dan 4.7% untuk *antena array 4x1*.

ACKNOWLEDGEMENTS

Firstly, I would like to express my sincere gratitude to my supervisor, Dr. Tarik bin Abdul Latef. His guidance and knowledge were invaluable to me throughout the development of this thesis. He also has motivated me to perform to the best of my abilities and made sure that I understand the concepts throughout the project duration.

I also would like to convey my appreciation to the dedicated staffs of the Deputy Dean's office (Postgraduate Studies) of Faculty of Engineering for their administrative services, information and guidance in the preparation of this research report. Special thanks are also dedicated to Shah Erawati and Nurhazirah for their guidance.

I could not end this acknowledgement without conveying heartfelt thank you to my beloved father and sisters for their endless moral and financial support throughout my academic years and personal growth.

TABLE OF CONTENTS

CHAPTER 3: METHODOLOGY

CHAPTER 4: RESULTS AND DISCUSSIONS

CHAPTER 5: CONCLUSION

REFERENCES

APPENDICES

LIST OF FIGURES

LIST OF TABLES

CHAPTER 1: INTRODUCTION

1.1 Background

Development in wireless technologies creates new opportunities for Body-Centric Wireless Communication (BCWC) which have gained huge attention among researchers and industry players due to their promising applications in personal healthcare, military, sports and body-sensor networks. Body centric wireless communication link between on-body electronic devices and surrounding environment can be established with the help of antennas. BCWC can be classified into three types based on the positions of the transmitter and receiver [1]:

- Off-body: Channel is off the body and in the free space and only one antenna in the communication link is located on the body.

- On-body: Most of the communication channel is on the surface of the body and both transmitting and receiving antennas are mounted on the body.

- In-body: Significant part of the channel is integrated into the body and implantable antennas are used.

There are two primary challenges need to be considered by researchers for antenna design for body-centric communication. The first challenge is to deal with degradation in radiation efficiency, radiation pattern, gain and the shift in input impedance of the antenna due to antenna-body interaction. Conventional antennas such as dipole [2], loop [3, 4], planar inverted-F (PIFA) [5, 6] and microstrip patch [7-9] were used for body- centric communications. The loop antenna is an omnidirectional antenna which gives maximum radiation along the loop's surface with E and H fields being perpendicular to each other [10]. A compact PIFA antenna has been designed for 2.4 GHz applications in [5] which also gives

an omnidirectional pattern. Patch antenna is a directional antenna that radiates power strongly in specific directions. This characteristic of patch antenna enables it to be suitable for on-body antenna design because maximum power need to be radiated away from the body. Besides that, microstrip patch antennas have been a popular candidate for wireless application due to their planar configuration and can be easily fabricated onto a printed circuit board (PCB).

The second challenge is an antenna's performance can be affected due to the strong coupling between the antenna and the human body which may influence the user's health. Therefore, preventive or corrective measures should be implemented to ensure that its performance does not change severely.

1.2   Problem statement

The purpose is to initiate communication with the body wireless is to provide the user with comfort and flexibility instead of bulky and wired connection. Wireless Body Area Network (WBAN) technology involves multiple sensor nodes located in-body or on-body which facilitates in monitoring the surrounding environment. The data from the sensors will be wirelessly transferred by antennas to an external computing facility. The antennas for body-centric communication should be low profile, compact in size and insensitive to the user's body proximity.

Although microstrip patch antenna of single element has been a promising candidate for body centric communication, it also suffers from several drawbacks such as narrow bandwidth and low gain. Thus, to enhance the bandwidth and gain of the antenna, multi-elements known as an array of single patch antenna can be designed. Furthermore, the study of human body's influence on antenna performance is crucial because human body anatomy

is unique for each individual. Behavior of electromagnetic waves propagating in the vicinity of human body are determined by the thickness and composition of the body tissue. This is because each body tissue has its own electrical property so variation in tissue thickness will influence the ways the waves are reflected and absorbed. The single element and array antennas proposed in this project is designed to operate for 2.4 GHz applications. An investigation on the antenna's performance both in free space and on-body for various tissue thickness are also investigated.

1.3   Aim and Objectives

The main aim of this project is to design on-body antennas that operate at 2.4 GHz Industrial, Scientific and Medical (ISM) band. To accomplish this aim, the objectives of this project include:-

1. To design and compare single element, 2x1 array and 4x1 array antenna's performance both in free space and on-body.

2. To investigate the influence of various tissue thickness on antenna's performance.

3. To improve on-body antenna's gain by adopting simple gain enhancement techniques.

CHAPTER 2: LITERATURE REVIEW

2.1   Introduction

The basic concept of microstrip antenna is explored here. In the beginning of the chapter also, wireless standards for body-centric communication antenna has been reviewed. Antenna material characterization, feeding mechanism and also the concept of multi-elements and its feeding technique also has been considered. Last but not least, the importance of determining parameters of tissue layers is also discussed.

2.2   Frequency Allocation for WBAN

The Institute of Electrical and Electronics Engineers (IEEE) 802.15 Task Group 6 authorized a dedicated standard termed IEEE 802.15.6 for Body Area Network (BAN) in 2012. It constitutes the physical (PHY) and medium access control (MAC) layers specified for short-distance wireless transmission in the vicinity of, or integrated into a human body (but not limited to humans) for various applications such as healthcare monitoring for the children or elderly, military or non-medical related. The requirements for BAN are the nodes have to be simple, economical in terms, cost, consume low power and guarantee its users of comfort. Thus, the standard features include three physical layers such as Narrowband (NB), Ultra-Wide Band (UWB) and Human Body Communications (HBC). Figure 1 depicts a spectrum allocation chart for all available frequencies for BAN applications.
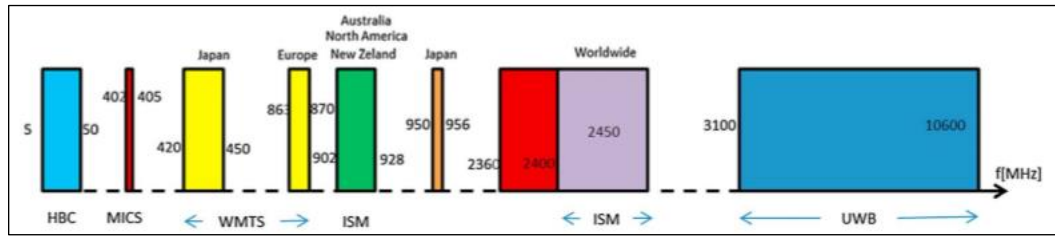
Figure 2.1: Allocation of WBAN frequency bands in different countries [11]

The requirement for high data rate is crucial in medical application because a huge amount of patients' data needs to be uploaded and transferred to the base station. The data rate requirement for WBAN varies from 1 kbps to 1 Mbps. Furthermore, antenna design for transmission and reception of data purposes has to be compact as to be possible. This can be achieved by using higher frequency bands for antenna design as size is inversely proportional to wavelength. Table 2.1 summarizes the characteristics of popular wireless standards for medical application.

Table 2.1: Features of medical wireless technology

Wireless Technology	Description
ISM Band	• Frequency ranges from unlicensed 902 - 908 MHz, 2.4 - 2.45 GHz, 5.7 - 5.8 GHz • Easy to install and access, low power utilization, cost effective • Congested due to wireless coexistence
MedRadio or MICS	• Frequency ranges from 402 - 405 MHz • Implantable antenna or devices are designed to work with this band • Limitations in transmitting the signal as it has very low power • Maximum EIRP : 25 µW at 3m from MICS devices
UWB	• Bandwidth exceeds 500 MHz, which provides high data rate • Low power consumption and complexity • Can penetrate through obstacles easily

2.3 Microstrip Patch Antenna

Microstrip antennas are desirable over other type of antenna configurations due to the distinctive characteristics such as low profile and flexibility in terms of resonant frequency, propagation, far-field pattern, impedance matching when the specific radiator shape and mode are selected. Additionally, they are also flexible to planar and nonplanar surfaces, inexpensive to fabricate them by exploiting the cutting edge printed-circuit engineering, and mechanically powerful when mounted on inflexible surfaces, suitable with MMIC designs [10]. A conventional microstrip patch antenna is built by integrating a dielectric substrate between radiating patch at the top and the ground plane as portrayed in Figure 2.2. The radiating element and ground plane is usually fabricated by using conductive metals such as copper or gold while the dielectric substrate is made of non-conducting material such as a FR-4 board.
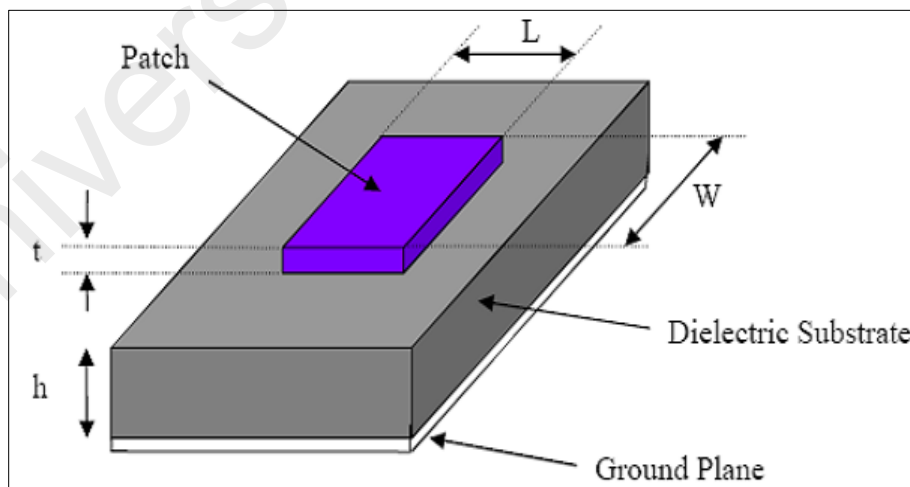
Figure 2.2: Microstrip patch antenna [10]

Furthermore, the radiating patch can be constructed using various shapes as illustrated in Figure 2.3. However, rectangular and circular structure are preferred by researchers because they are really suited for thin substrates. Rectangular configuration is distinguishable and simple to evaluate for practical engineering. The antennas in this research are rectangular in shape to simplify the fabrication process.
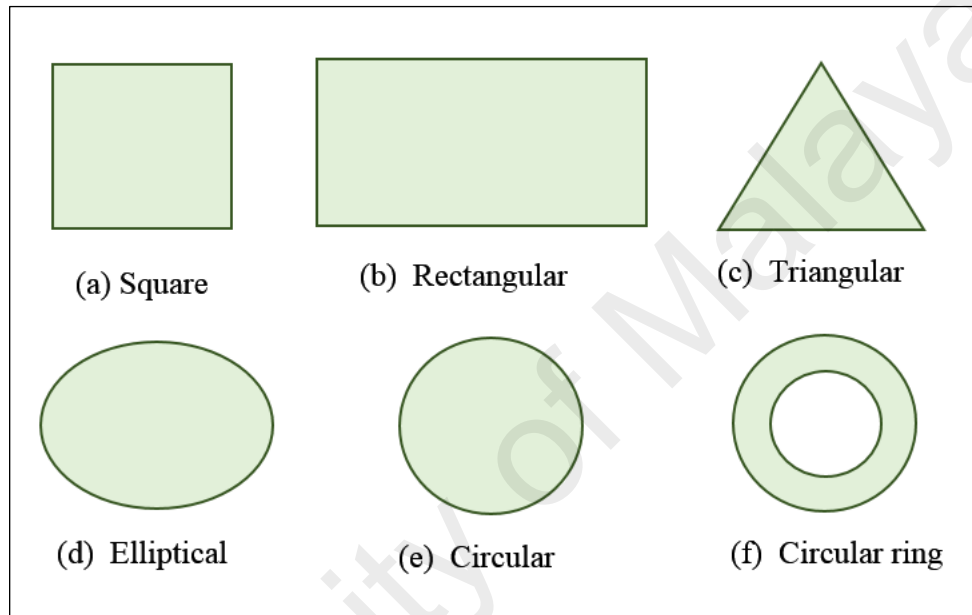
Figure 2.3: Typical configurations of patch antennas

Microstrip patch antenna also suffers from several drawbacks despite being simple in structure, low profile and moderate in size. The disadvantages are low efficiency, low power, polarization purity is difficult to achieve, excitation of surface waves and narrow frequency bandwidth.

2.4   Feeding Mechanism

Various approaches can be taken to feed the microstrip antennas. These techniques can be divided into contacting and non-contacting [10]. Power is supplied directly to the radiator using direct path of transmission lines such as transmission feed line, coaxial and inset feed

7

in the contacting technique. Electronic coupling facilitates power transmission between the feed line and the conducting element in the non-contacting technique. The four most popular feeding techniques are feed line, coaxial, inset-feed and proximity coupling. However, only feed line, inset –feed and coaxial feeding method will be reviewed in this research.

2.4.1 Transmission Line

A smaller in width radiating strip compared to the patch is linked to the edge of the plot as exhibited in Figure 2.4. Such method allows the feed line and patch to be etched on substrate resulting in a planar structure. The feed line can be directly connected to the patch for the purpose of impedance matching. Its location and measurement can be adjusted to result in desired impedance matching as well. Therefore, the transmission line feed simplifies the modelling and fabrication process.
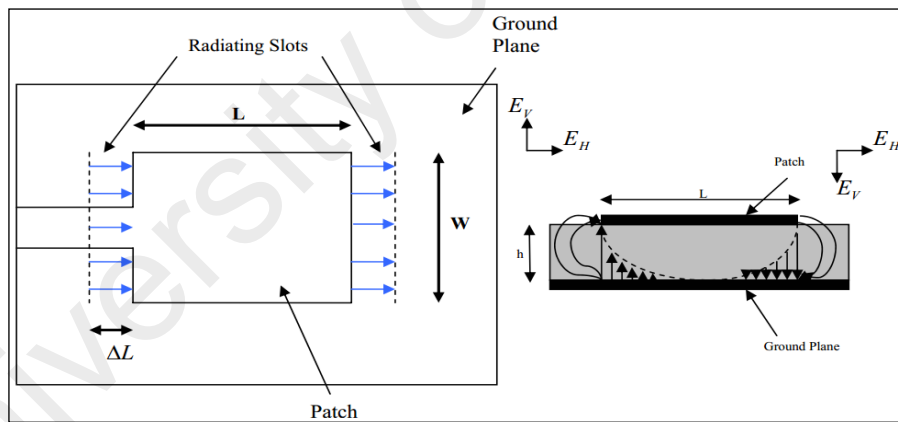
Figure 2.4: Transmission line feed [10]

2.4.2 Inset-Feed

Impedance of the feed line can be equated to the path without the aid of any extra matching device with the creation of inset cut in the patch as displayed in Figure 2.5. The matching can be done by adjusting the inset location. It is easy to fabricate such simple feeding configuration and also provides good impedance matching of the antenna. In this

study, the authors found that the inset-feed contributed the best result in terms of gain and reflection coefficient compared to strip line and quarter- wave feed [12].
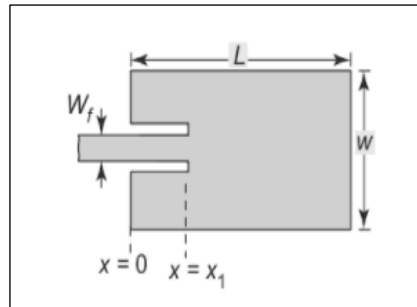
Figure 2.5: Recessed inset-feed line [13]|

2.4.3 Coaxial Feed

The inner conductor of the coaxial connection is connected to the radiator, while the outer part is linked to the ground as depicted in Figure 2.6. The benefits of this type of feeding include it can be located at any preferred position, resulting in good impedance matching and low spurious radiation. This feed is also easy to construct, making this technique to be popular among researchers.
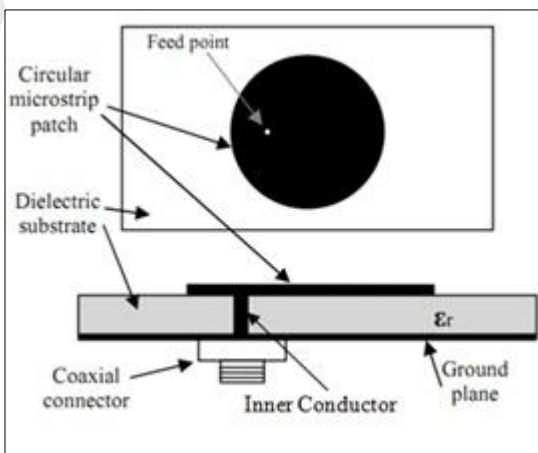
Figure 2.6: Coaxial-probe feed [10]|

The major drawback of probe-feed concept is that the connector sticks up from the antenna plane, which is impractical for on-body applications. The antenna will be mounted on the human body and thus, should not bring discomfort for the person who wearing the antenna in terms of physical orientation. Additionally, the antenna should be of a flat and planar configuration. Therefore, the inset-feed is chosen to feed the antennas.

2.5   Antenna Material Specification

Antenna's performance is dependent on features of the materials used to develop them. For this reason, it is really important for an antenna designer to have a good understanding of the electrical properties of both conductive and non-conductive material that are readily available in the market. After analyzing the electrical characteristics such as dielectric constant and conductivity, suitable materials are selected to design antennas with good radiation property and efficiency.

2.5.1   Substrate Materials

Antennas designed for on-body application should transmit energy perpendicular to the flat structure and the ground plane and systematically protects the human body. Thus, the radiation strength of the antenna is distinctively influenced by substrate's dielectric constant and thickness. Generally, low value of dielectric constant reduces surface wave losses that are fixed to guided wave transmission within the substrate. Dielectric substrate's thickness is also vital for antenna design. The substrate that results in excellent antenna performance are thick substrates with low electrical permittivity as it provides a large bandwidth. In addition to it, a substrate with low loss tangent is also preferred to design high-gain antenna. The

electrical properties and features of the substrate materials used in this research is described
in the Table 2.2.

Table 2.2: Electrical properties of substrate materials

Properties	RT Duroid 5880	R0 3730	FR - 4
Dielectric constant, ε_r, 10 GHz, 23 °C	2.20 ± 0.02	3.00 ± 0.06	4.3 - 4.7
Dissipation factor, $\tan \delta$ 10 GHz, 23 °C	0.0009	0.0016	0.0025

2.5.2 Conductive Materials

The choice of conductive metals for both patch and the ground plane also plays a
substantial role to guarantee efficient performance of the proposed antennas. Copper, gold,
silver and other metals are few conducting materials that available for commercial purposes
today. Conductive material with very low value of electrical surface resistivity is usually
chosen to reduce the antenna's electrical losses.

2.6 Microstrip Antenna Arrays

Single element antenna gives broad radiation pattern in which the directivity and gain
values are relatively low. Although directivity and gain can be increased by enlarging the
size of the antenna, the main beam becomes narrower. As a consequence, side lobes also gets
larger. Since large antennas limit its performance, array configuration can be utilized.
Generally, the elements of an array are indistinguishable.

An array's total field can be derived mathematically through vector addition of the
individual element's field. It is expected that the amount of current flowing in each element

11

is the same which is influenced by the distance between the elements and type of feeding network. Five attributes can be tuned to obtain radiation pattern which are:

- Geometrical structure (circular, rectangular and etcetera)

- Spacing between antenna elements

- Excitation phase of respective elements

- Excitation amplitude of respective element

- Pattern of individual elements

Multiple single elements can be arranged in a certain orientation to form an array of antennas as highlighted in Figure 2.7. The goal of array design is to obtain the highest antenna gain and directivity with minimal side lobe level. However, the arrangement of the elements to form an array network is crucial for it to be successful.
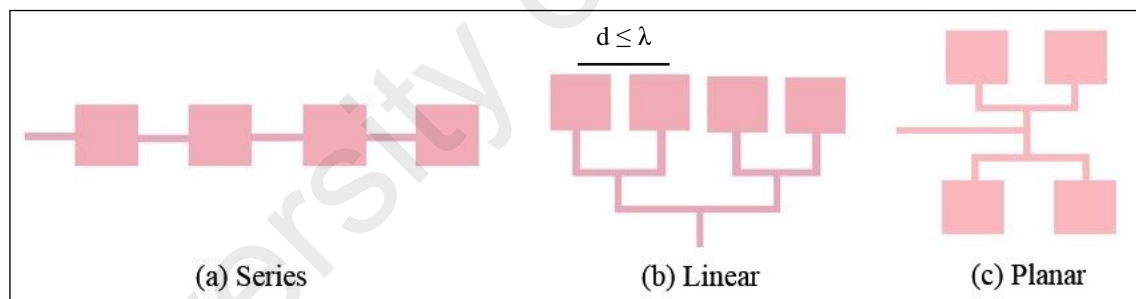
Figure 2.7: Typical array antenna arrangement

As Figure 2.7 (a) indicates, a single line is adequate to feed the elements which is also labeled as series-feed network. This technique is restricted to fixed- beam arrays or beam –scanning arrays through frequency variation.

Linear array in Figure 2.7 (b) consists of N elements arranged along a line. The spacing between the elements can be classified into two: equal or unequal. Number of elements to put in a design primarily depends on the designer's preference. Equally spaced linear array

is also termed as uniform array in which all the identical elements have same amplitude and excitation phase.

In addition to the linear orientation of radiators, they also can be arranged in a grid to form a planar array. Planar arrays are more functional as they provide a symmetrical radiation pattern with smaller side lobes. Thus, it is more convenient to control the antenna beam with this configuration. An antenna designer should emphasize on the distance between each element while designing a series, linear or planar antenna which distance (d) ≤ lambda (λ) is adapted. If $d > \lambda$, this will result in grating lobes in the antenna pattern. Grating lobe is identical to the main beam but it is projected in an unintended direction. This research utilizes linear arrangement of the antenna design.

2.6.1 Feeding Networks for Array Antenna

As discussed in the previous section, series elements can be fed by deploying a single line. The second feeding technique involves multiple lines that is corporate-feed network. Corporate-feed method splits power by $2^n = 2$, 4, 8 and etcetera. Implementation of this technique provides the designer with freedom in controlling the amplitude and phase of each element. The corporate-feed can be realized through the use of T-junction or Wilkinson power divider.

2.6.1.1 Corporate Feed Configuration

If the transmission line loss is not taken into account, the T-junction can be considered lossless. Thus, such junctions cannot be jointly matched to all ports. Power division is done to ensure that equal power distribution among the N elements. Microstrip lines of different impedance are considered for matching purposes. Hence, the arrangement

13

in Figure 2.8 (a) is applied for 2x1 linear array design that is for input 50 Ω line splits into two output 100 Ω lines. The Wilkinson power divider technique allows matching of all ports and isolation between output ports. This equal-split divider can be designed for 50 Ω input impedance system by using a quarter - wave transformer to match the 50 Ω feed line to 100 Ω lines. Figure 2.8 (b) is a good illustration of the Wilkinson power divider concept. Feed network of 4x1 array includes both T-junction and Wilkinson power divider.
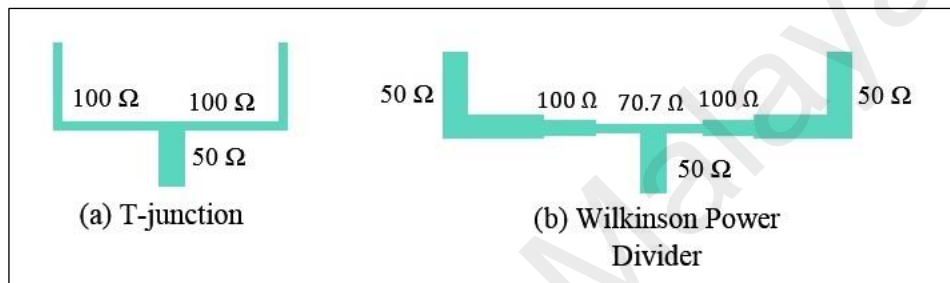
Figure 2.8: Microstrip line feed network

2.7   Study of Biological Tissue Thickness based on Previous Research Works

The influence of electromagnetic wave propagation through the human tissue dependent on thickness and dielectric characteristics of respective layers. The dielectric properties, conductivity and thickness of body tissue vary from an individual to another with age, gender and health conditions and also a particular region of the body. Furthermore, the operating frequency of the electromagnetic wave also influences permittivity, conductivity and penetration depth of the tissue layers. Penetrating microwaves will behave differently due to alteration in penetration depth for these reasons [14]:

- Electrical properties of body tissues depends on resonant frequency
- Outer tissues penetration depth will be affected by propagation of microwaves through different tissues

14

- Scattering characteristic of the tissue changes as lambda (λ) varies

Body tissue can be classified into two types: high-water content and low-water content [1]. Skin and muscles are some examples of the first type due to higher values of permittivity and conductivity while fats of low permittivity and loss belong to the second type. The skin organ covers the exterior of living organisms and acts as a barrier against surrounding environment. Its tissue includes the epidermis, dermis and hypodermis as evidenced in Figure 2.9. Hypodermis or subcutaneous adipose tissue (SAT) is located underneath dermis layer. It provides mechanical protection, thermoregulation and energy storage. Body region, age, gender and diet of an individual greatly affects the thickness of the fat layer. Muscle tissue is generally considered as elastic and responsible to produce and maintaining motion. Skeletal and cardiac muscles are able to contract and relax [3]. Therefore, it is necessary for a designer to identify complete compositions of tissue layers to develop efficient antennas for body-centric communication. The most common regions of human body preferred for on-body applications are arm, abdomen, chest or thigh. The configuration and thickness of several tissue layers of different body parts reported in literature are compiled in Table 2.3.
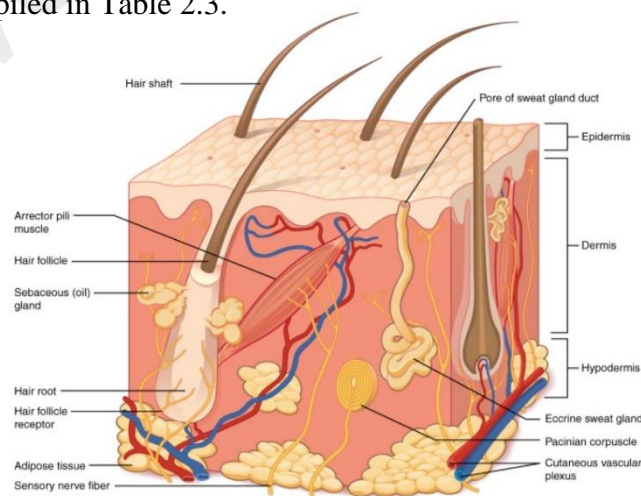
Figure 2.9: Composition of human skin [15]

Table 2.3: Human tissue thickness according to different body region

Reference	Application	Gender	Tissue Model Configuration	Body Parts	Thickness of body tissues (mm)		
					Skin (dry)	Fat	Muscle
[5]	ISM (2.4GHz)	Man	Rectangular	Chest	4.5	2/4/10/8	Not stated
[16]	5.6 GHz	Not stated	Rectangular	Chest	2	10	28
			Cylindrical	Arm			
[3]	ISM (433 MHz)	Adult	Rectangular	Frontal Thorax	0.96	15	13.5
[4]	MICS (401-406 MHz) ISM	Not stated	Cylindrical	Not stated	4	4	52
[6]	MICS (403.5 MHz)	Not stated	Rectangular	Chest	3	6	26
				Abdomen	2	8	25
[17]	Not stated	Male (Taro)	Rectangular	Abdomen	2	9	7
[7]	ISM (2.45 GHz)	Not stated	Rectangular	Not stated	2	4	44
[8]	ISM (2.45 GHz)	Not stated	Rectangular	Not stated	1	2	10
[9]	ISM (2.45 GHz)	Not stated	Rectangular	Not stated	1	2	30
[2]	ISM (2.45 GHz)	Not stated	Rectangular	Not stated	4	4	8
[18]	MICS (404 MHz)	Not stated	Rectangular	Not stated	5	13	35
[19]	MICS (402-405 MHz)	Not stated	Rectangular	Chest	3	4	20

Reference	Application	Gender	Tissue Model Configuration	Body Parts	Thickness of body tissues (mm)		
					Skin (dry)	Fat	Muscle
[20]	MICS (402-405 MHz)	Not stated	Rectangular	Trunk	4	4	20
[21]	ISM	Not stated	Rectangular	Not stated	3	7	60
[22]	BAN	Children	Rectangular	Frontal Thorax	0.6 - 1	0 - 16	30
		Adult			0.8 - 2.6	1.4 - 23.2	30
[23]	ISM (902-928)	Male	Rectangular	Not stated	1.6 - 3	0 - 15	20 and 25
[24]	1.38 GHz and 2.88 GHz	Female	Ellipsoidal	Chest	2	15	5
[25]	MICS (403MHz) ISM (2.45 GHz)	Not stated	Rectangular	Arm	4	4	16
[26]	0.9 - 17 GHz	Not stated	Rectangular	Not stated	1.5 - 2.5	0-23	0-30
[27]	2.45 GHz	Not stated	Rectangular	Not stated	2	4	30
[28]	Multiple	Not stated	Rectangular	Forearm	2	2	20
				Chest	3	3	20
				Thigh	4	5	20

CHAPTER 3: METHODOLOGY

3.1   Introduction

Antenna design process of single and multi-elements are discussed in detail in this chapter which includes material selection, calculation of the dimensions of both radiator and feed and optimization. Next, their performance is evaluated both in free space and on-body setting. This chapter also addresses several gain enhancement approaches to improve the interaction between the antenna and body tissue.

3.2   Project Flow

This project is organized into 5 phases which are:-

a) Review related literature on properties of the material, antenna suitable for on-body application, the concept of the antenna array and feeding mechanism

b) Further study on the actual thickness of tissue layers according to human body parts

c) Design single and array antenna at frequency of interest using transmission line method

d) Compare and contrast the variation in antenna's performance both in free space and human body environment

e) Investigate on the significance of gain enhancement techniques in improving antenna's performance of on-body

These phases will be further explained by stages as follows: -

Stage 1:

Studies are conducted to understand the key concept and requirement of body-centric wireless communication (BCWC). The selection of different laminate materials according to the conductivity, permittivity and their respective thickness are emphasized. Moreover, a study on antenna suited for on-body application also has been considered. Classification of antenna arrays and their design requirement cited in literature also has been referred.

Stage 2:

Factors such as age, gender, dietary status and the anatomy of an individual will influence the performance of the antenna. Therefore, knowledge of electromagnetic properties of the body tissues and their respective thickness is crucial. At this stage, several manuscripts in the literature are surveyed to obtain the actual thickness of the tissue layers which are validated according to body parts.

Stage 3:

Attention is focused on designing the rectangular microstrip patch antenna using three different substrate materials at 2.4 GHz. Dimensions of single element and array antenna are calculated and optimized to meet requirement.

Stage 4:

The dimensions of antennas that provide best results in terms of reflection coefficient, bandwidth, gain and etcetera are finalized. Thereafter, performance evaluation of antenna's on-body using three layer structure with uniform thickness respectively are carried out as a preliminary. The antenna configurations that results in low loss will be used to investigate the effect of the actual thickness of body tissue obtained from literature.

Stage 5:

The final step involves improving the performance of antennas that are mounted on-body by selecting an actual configuration of three-layer structure. The numerical results of gain enhancement will be elaborated in the next chapter.
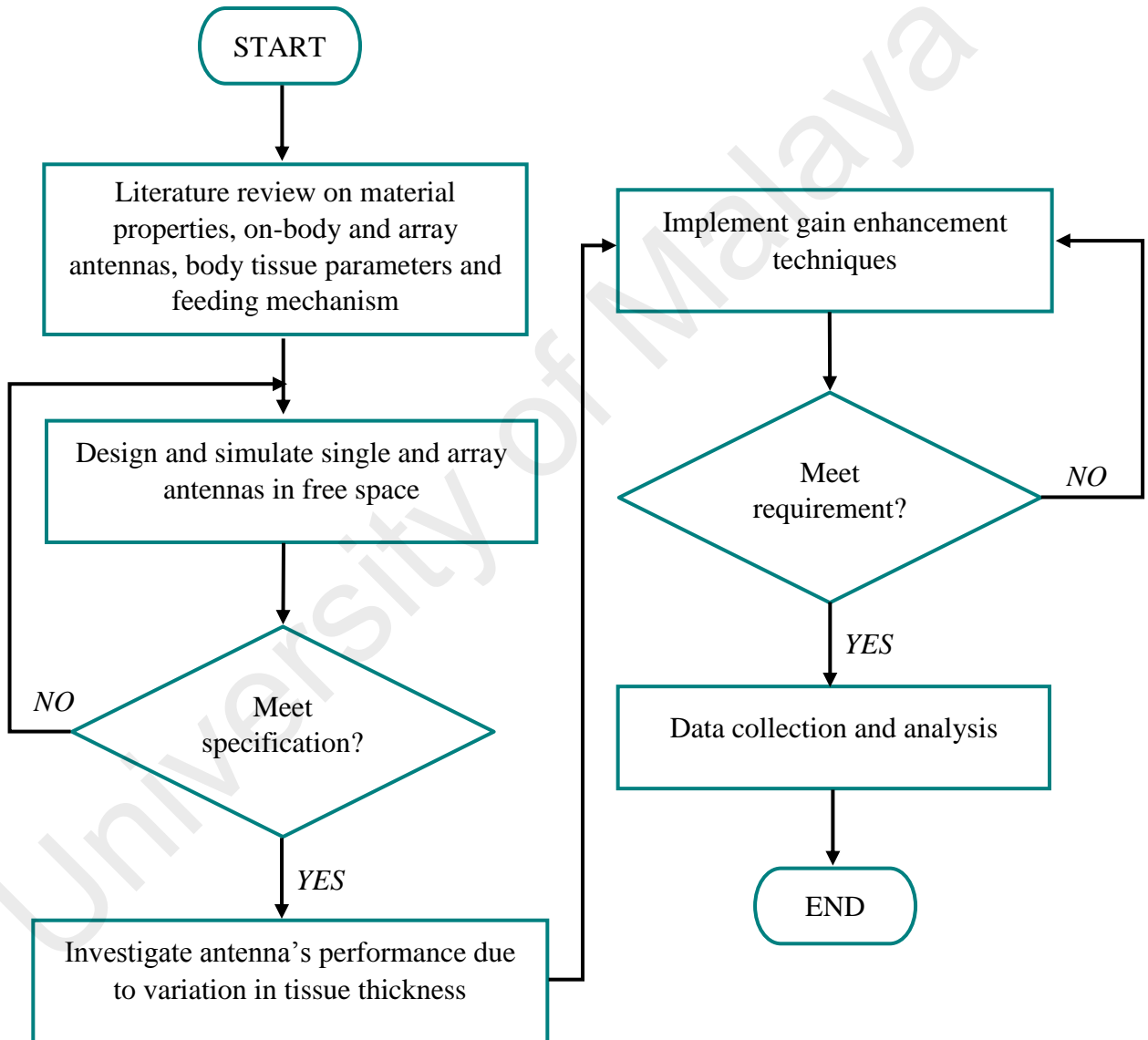
Figure 3.1: Project flowchart

3.3 Design Specification

3.3.1 Antenna Material Specification

The selected substrate materials should exhibit uniform dielectric constant, low loss tangent and acceptable thickness. Two dielectric materials of Rogers Corporation such as RT Duroid 5880 and R0 3730 are used in this research along with epoxy laminate, FR-4. The radiator and the ground plane are designed using conductive material such as pure copper. The specification of all materials used are listed in Table 3.1. Full material description of Roger's laminates can be found at Appendix A and Appendix B.

Table 3.1: Electrical properties of the dielectric and conductive materials

Material \ Parameter	RT/ duroid 5880	R0 3730	FR-4	Pure Copper	Aluminium
Dielectric constant, ε_r	2.2	3	4.7	-	-
Conductivity, S/m	-	-	-	5.96e+007	3.56e+007
Dissipation factor, tan δ	0.0009	0.0016	0.0025	-	-
Thickness, h (mm)	1.6	1.534	1.6	0.035	1

3.3.2 Design Methodology

The initial parameters and dimension of a single rectangular patch antenna can be computed based on Transmission Line Model equation. The width of the patch for specific resonant frequency, f_r is determined using equation 3.1:

$$W = \frac{c}{2 f_r} \sqrt{\frac{2}{\varepsilon_r + 1}} \qquad (3.1)$$

21

Since the edges of the patch will experience fringing effect, some of the lines of electric field will pass through the air instead of the substrate medium. Therefore, modification need to be done to the relative permittivity whereas physical length of the patch is also extended from its original configuration. The effective dielectric constant, ε_{eff} and the extended incremental patch length, ΔL are given by

$$\varepsilon_{eff} = \frac{\varepsilon r + 1}{2} + \frac{\varepsilon r - 1}{2}\left(1 + 12\frac{h}{w}\right)^{-\frac{1}{2}} \tag{3.2}$$

$$\Delta L = 0.412h \; \frac{(\varepsilon eff + 0.3)(\frac{w}{h} + 0.264)}{(\varepsilon eff - 0.258)(\frac{w}{h} + 0.8)} \tag{3.3}$$

Thus, the accurate patch length is calculated through equation 3.4 as shown:

$$L = \frac{c}{2f\sqrt{\varepsilon eff}} - 2\Delta L \tag{3.4}$$

The patch requires characteristic impedance of 50 Ω for its feed line. Therefore, inset-feed method can be used to equate the input resistance to the feed. First, conductance, G_1 and mutual conductance, G_{12} must be computed to obtain input resistance as stated in equation 3.5 and equation 3.6:

$$G_1 = \frac{1}{120\pi^2}\int_0^\pi \left[\frac{\sin\left(\frac{k_0 W}{2}\cos\theta\right)}{\cos\theta}\right]^2 \sin^3\theta \; d\theta \tag{3.5}$$

$$G_{12} = \frac{1}{120\pi^2}\int_0^\pi \left[\frac{\sin\left(\frac{k_0}{2}\cos\theta\right)}{\cos\theta}\right]^2 J_0\left(k_0 \; L\sin\theta\right)\sin^3\theta \; d\theta \tag{3.6}$$

Where, J_o is the Bessel function of the first kind of order zero while k_o is wavenumber.

Next, the input resistance is then obtained by

22

$$R_{in} = \frac{1}{2\,(G_1 + G_{12})} \tag{3.7}$$

Finally, the input resistance at $y = y_o$ from the edge can be computed using equation 3.8:

$$R_{in}\,(y_0) = R_{in}\,(0)\,cos^2\left(\frac{\pi}{L}y_0\right) \tag{3.8}$$

At y_o, matching is made as the input resistance is 50 Ω. The inset feed length, y_o can be solved using Matlab solver.

3.4   Antenna Design in Free Space

3.4.1 Single Element Design

In the previous section, procedures to determine patch length and width and inset feed length for single element are described. The calculated dimensions are tabulated in Table 3.2.

Table 3.2: Dimensions of single patch antenna

Parameters	Values (mm)		
	RT Duroid 5880	R0 3730	FR - 4
Patch length,Lp	49.4	44.2	29.6
Patch width,Wp	41.3	35.6	37.02
Feed length,Lf	23	20.1	17.29
Feed Width,Wf	4.93	3.86	3.137
Inset feed,yo (50 ohm)	14.503	12.74	9.96
Inset feed,yo (100 ohm)	11.55	10.36	8.995

CST Microwave Studio software is used to design and optimize all antenna configurations. The final dimensions of proposed single patch antenna for RT Duroid 5880 and R0 3730 substrates are illustrated in Figure 3.2. Final geometry of single- element antenna using FR-4 can be acquired from research findings of previous candidate. It is worth mentioning that both substrate and ground share the same dimension that is 80 mm x 80 mm.
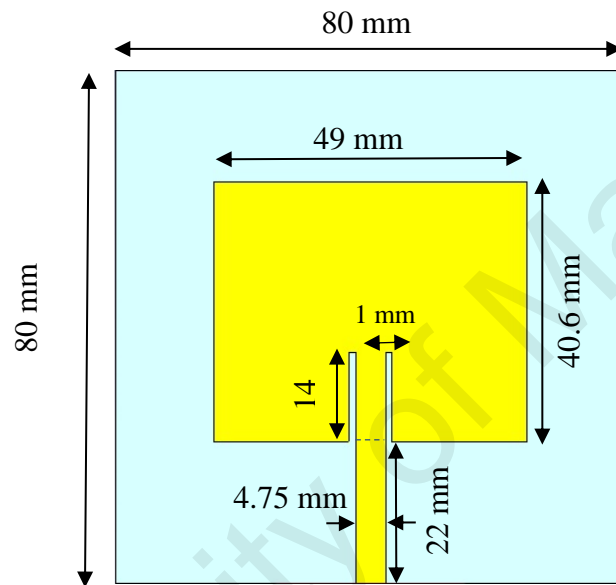
(a) RT Duroid 5880
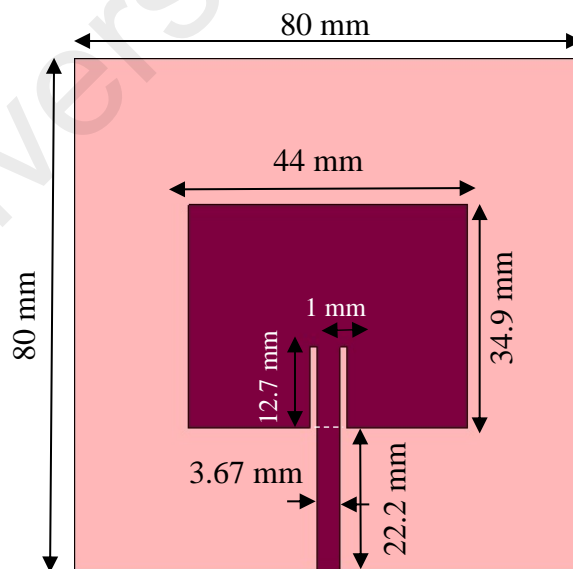
(b) R0 3730

Figure 3.2: Front view of single patch antenna

3.4.2 Array Antenna Design

3.4.2.1 Array Antenna for FR – 4

Selection of number of elements and separation between them is imperative in maximizing the performance of a linear antenna array. Figure 3.3 displays structure of 2x1 and 4x1 linear array with 0.5λ spacing respectively. Patch elements are also configured in grid manner as portrayed in Figure 3.4. The both arrays are designed with length and width of each element is intriguingly identical to the single patch design. To design four element array, 50 Ω need to be matched to 100 Ω transmission line by determining the characteristic impedance. It can be calculated by

$$Z_c = \sqrt{Z_0 R_{in}}$$ (3.9)

$$= \sqrt{(50\Omega)(100\Omega)}$$

$$= 70.71 \ \Omega$$

The impedance calculation for 50 Ω, 70.71 Ω and 100 Ω feed line is outlined in Table 3.3.

Table 3.3: Feedline impedance computation

Material	Impedance (Ω)	Dimension (mm)	
		Length	Width
FR - 4	50	17.29	3.137
	70.71	17.1	1.52
	100	17.5	0.7
RT Duroid 5880	50	23	4.75
	70.71	23.2	2.83
	100	23.6	1.43
RO 3730	50	20.1	3.67
	70.71	20.5	2.15
	100	20.9	1.03
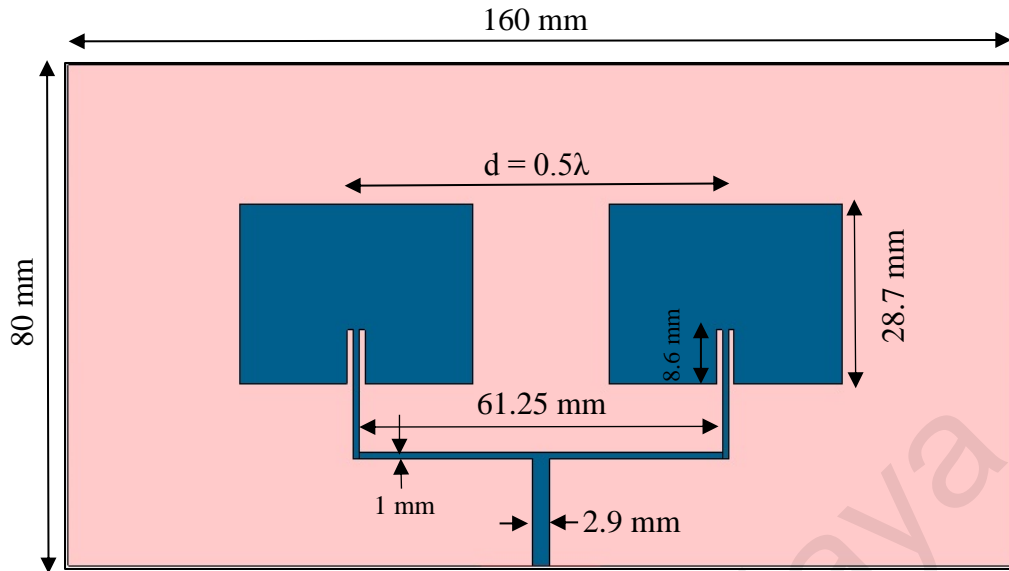
(a) 2x1 Array
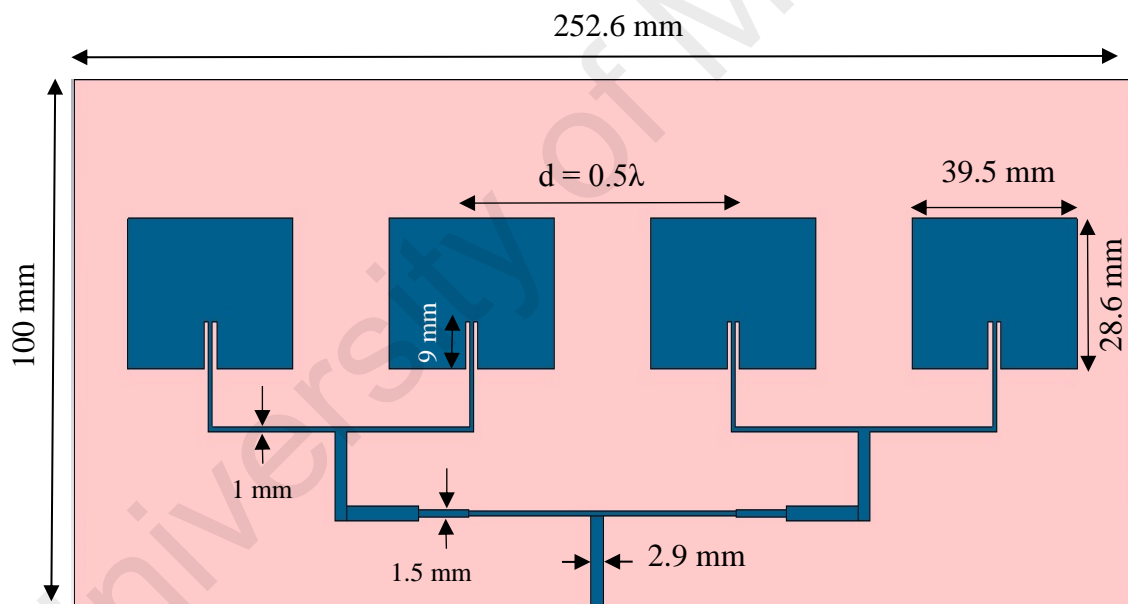
(b) 4x1 Array

Figure 3.3: Geometry of array antenna for FR-4 substrate
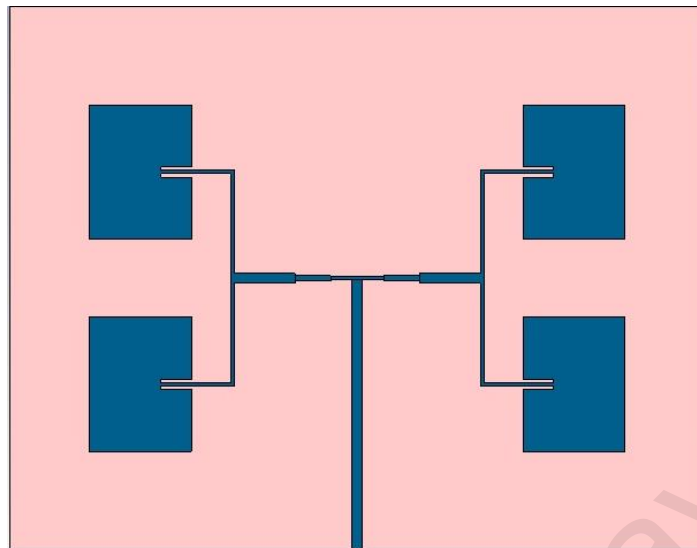
Figure 3.4: 2x2 array antenna for FR-4 substrate

3.4.2.2 Array Antenna for RT Duroid 5880

Array of 2 and 4 elements arranged in linear manner are designed using RT Duroid 5880 with the same design procedure for comparison purposes. Figure 3.5 highlights the dimensions of array antenna.
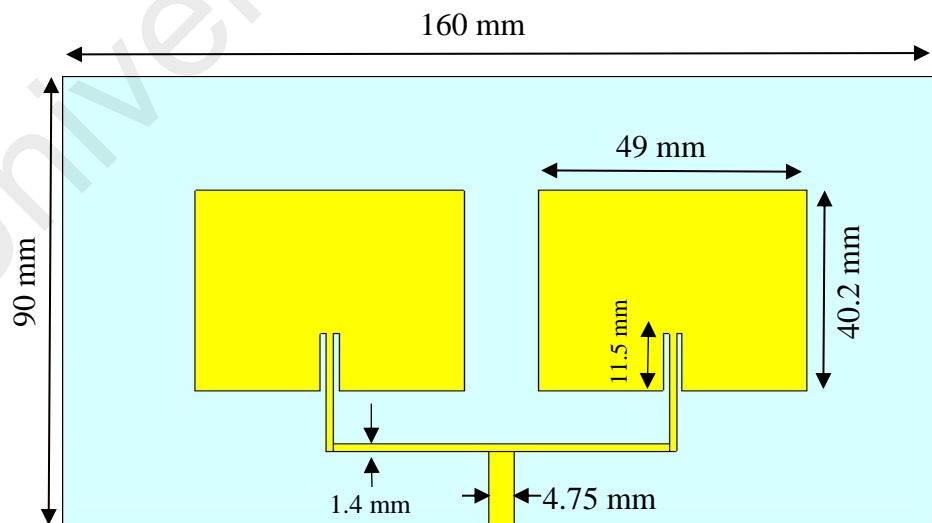
(a) 2x1 Array
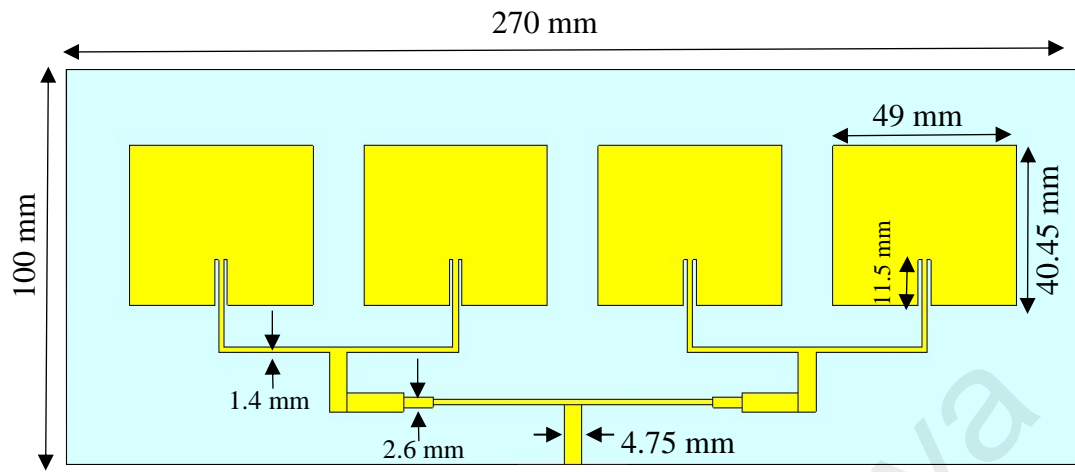
(b) 4x1 Array

Figure 3.5: Design specification for RT Duroid 5880 antenna array

3.4.2.3 Array Antenna for R0 3730

Figure 3.6 represents architecture of 2x1 and 4x1 linear array for R0 3730 also with 0.5λ spacing.
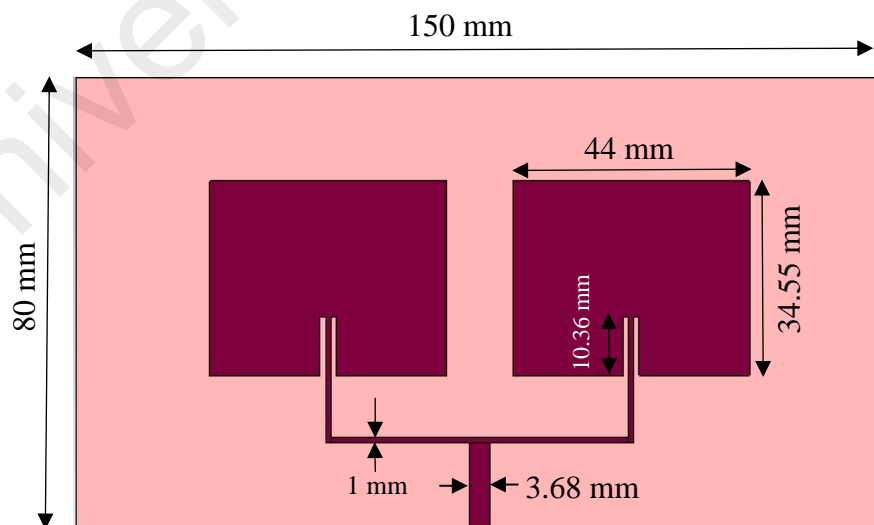
(a) 2x1 Array
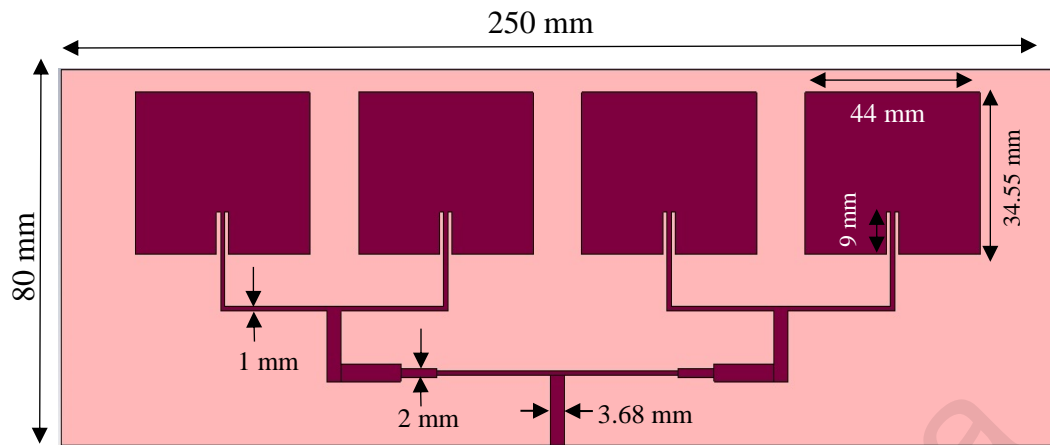
(b) 4x1 Array

Figure 3.6: Geometry of array antenna for R0 3730 substrate

3.5   Antenna Design for On-Body Communication

The proposed antennas are placed on three-tissue layer that represents human body model as visualized in Figure 3.7. The electrical properties of the tissue layers can be obtained from database [29, 30] and are stated in Table 3.4. A uniform thickness 3mm is considered for the skin, fat and muscle tissue respectively to investigate the interaction of electromagnetic waves with biological tissues. The dimensions of tissue layers are set equal according to antenna configurations.

Table 3.4: Electrical properties of body tissues at 2.4 GHz

Tissue Type	Relative permittivity	Conductivity (S/m), σ	Penetration depth (mm)
Skin (Dry)	38.1	1.441	23
Muscle	52.7	1.705	23
Fat	5.285	0.102	119.6
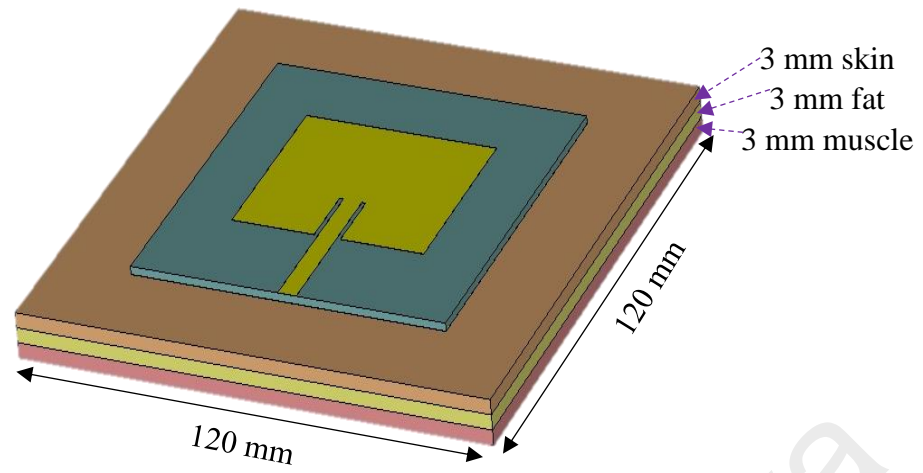
(a) Single element
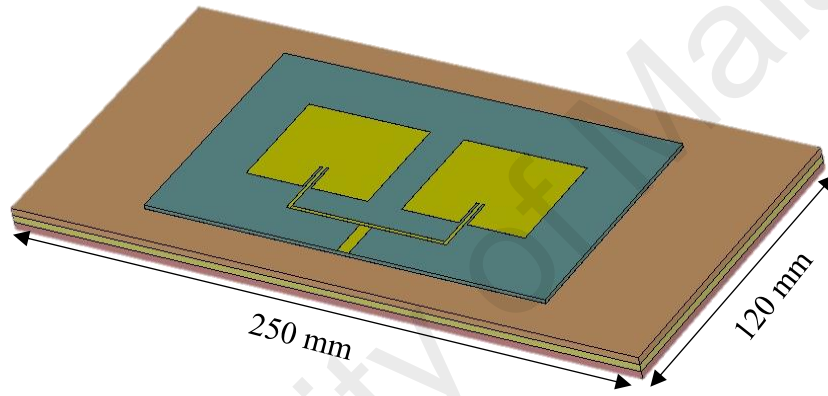
(b) 2x1 array
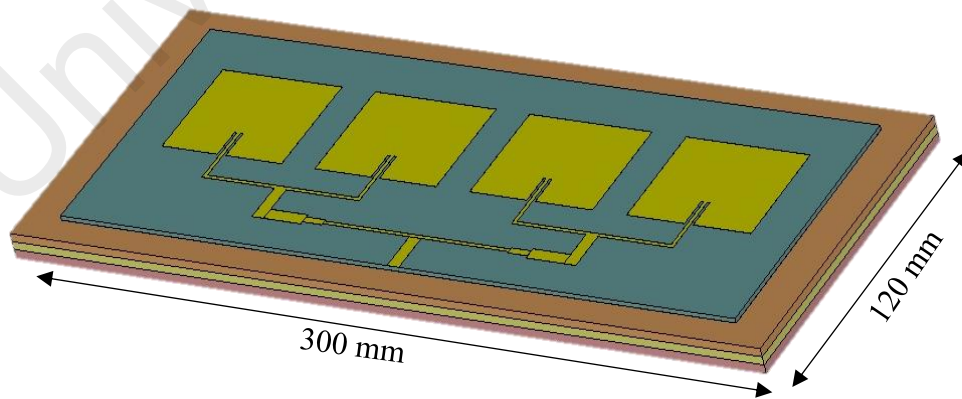
(c) 4x1 array

Figure 3.7: Antennas on human body tissue for RT Duroid 5880 substrate

30

3.5.1 Parametric study of variation in body tissue thickness

Based on the preliminary antenna simulations for on-body setting, it is discovered that RT Duroid 5880 provides low gain loss comparatively. Therefore, antennas designed using that substrate will be used to evaluate its performance on-body with actual thickness of body tissues. Based on literature, the thickness of human skin ranges from 1mm to 5 mm depending on body regions. Variation in muscle and fat tissue thickness is related to factors such as age, gender, nutritional status and body parts of an individual. In addition, subcutaneous adipose tissue thickness also changes with Body Mass Index (BMI). It is ratio of amount of body lipid correlated to height and weight of individual. Table 3.5 reports the thickness of fat tissue according to BMI classification.

Table 3.5: Hypodermis Layer in the Chest near Shoulder Area of People with Different BMI [31]

BMI	Man Hypodermis (mm)	Woman Hypodermis (mm)
Underweight	<3	<7
Normal	3-5	7-10
Overweight	6-16	11-20
Obese	>16	>20

Muscle thickness is considered to be variable parameter that ranges from 7 mm [17] to 60 mm [21]. This research focuses on designing antennas to be placed on chest of an adult. Parametric analysis is carried out by setting the skin thickness for 2 mm, 3mm and 4.5 mm while the muscle layer is labeled as 20 mm thick. The thickness of fat tissue is assigned according to BMI classes respectively: 2mm/4mm/10mm/18mm for man and 3mm/9mm/15mm/21mm for woman.

3.5.2 Gain Enhancement Techniques for On-Body Antennas

Transmission line are critical part of antenna design as it is used for the purpose of impedance matching and minimize power loss from the antenna. Antenna reactive fields interact with the body resulting in degradation of input impedance, gain and efficiency. Therefore, modification is done to the transmission line in Figure 3.8 by blending the edge as indicated in Figure 3.10 to improve impedance matching and gain. Note that the tissue thickness is assigned as 9 mm for the original structure. Different approach has been proposed in this research to overcome the disadvantage of antenna-body interaction by using the simple body model configuration in Figure 3.9. The thickness of body tissue is validated in [28].
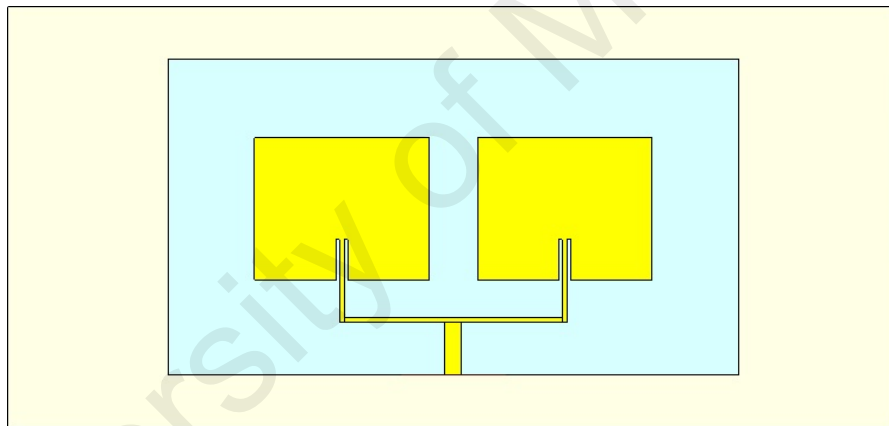
Figure 3.8: Original structure of 2x1 array antenna on-body
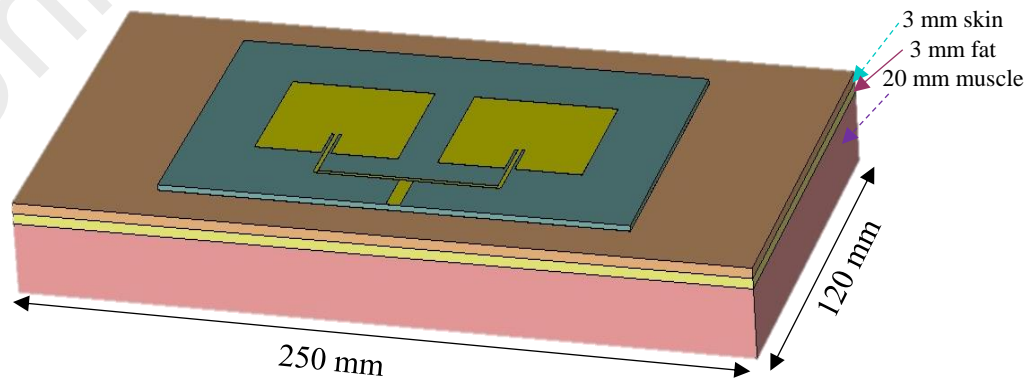
Figure 3.9: 2x1 array antenna on human chest model
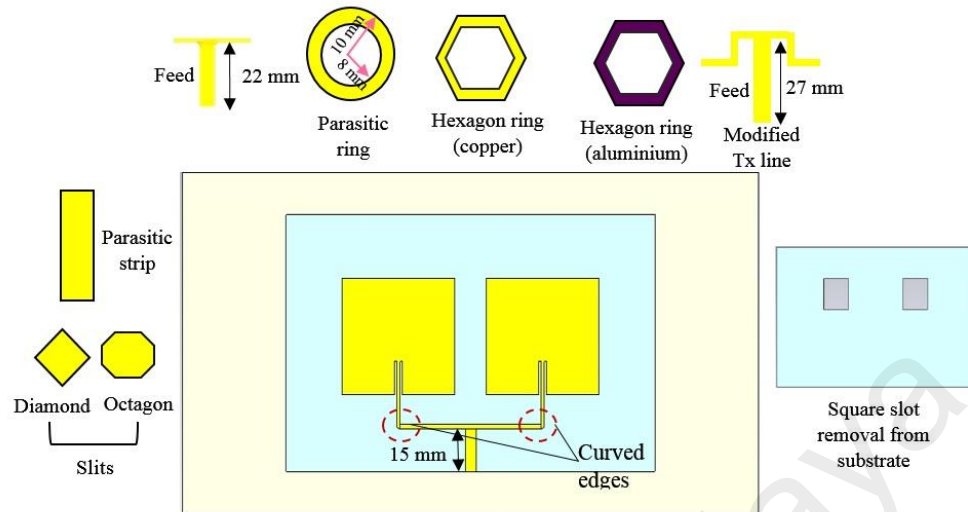
Figure 3.10: Modifications implemented on the design

Then, modification of feed structure are proposed by increasing its length from 15 mm to 22 mm. In addition, current path of antenna is also altered due to adjustment of transmission line. The final dimension of feed length is 27 mm. Gain enhancement approach includes addition of superstrate for terahertz application [32] and usage of metamaterials such as EBG structure [33]. Superstrate is a dielectric layer of specific thickness placed on top of radiator which results in additional complexity. A recently reported work [34] proposed placement of hemispherical lens and parasitic ring on top of skin layer to improve the gain of an implantable antenna. The effectiveness of parasitic elements in increment of antenna gain for free space communication also has been discussed in [35]. Parasitic elements should be placed at optimum distance from driven element as it need to receive radiation from main radiator.

Two parasitic strips with dimension 12 mm x 36 mm are vertically placed 9 mm away from the main radiator. Since the type of material used to design parasitic elements and their shape may influence antenna performance, a circular parasitic ring with a radius of

33

10 mm and 2 mm wide is placed adjacent to the main feed in the earlier stage. The influence of different shape configuration is then investigated by replacing the circular ring with hexagon ring made of pure copper. Further experiment is also conducted by changing the materials of the hexagon ring from pure copper to another conductive material, aluminium. This antenna array is further modified by cutting four diamond slots, two at the parasitic strips and another two is at the dual patches and two octagon slots at the strips as well. Last but not least, two square slots of 20 mm x 20 mm dimension are also removed from the substrate. The final structure of proposed array antenna is displayed in Figure 3.11.
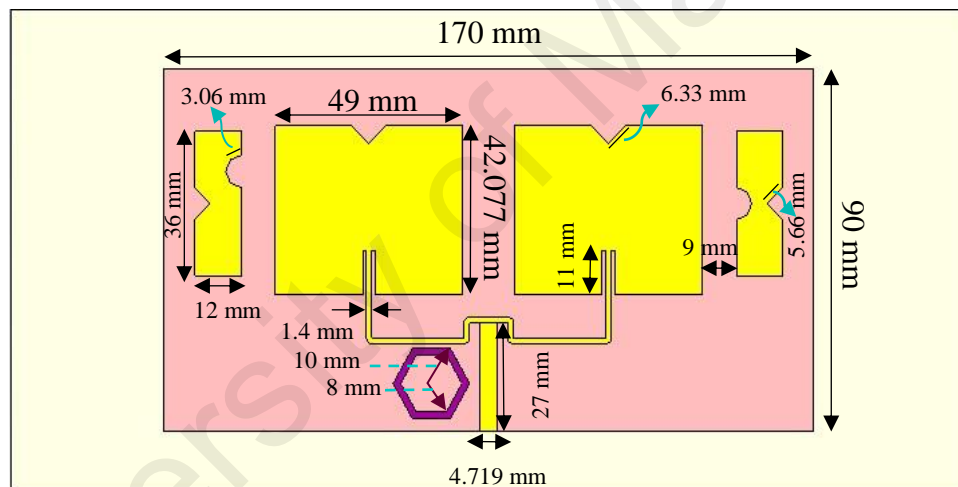
Figure 3.11: Final proposed geometry of 2x1 array on-body antenna

The authors in [35] investigated the effect of parasitic patches in multi-banding and gain enhancement of microstrip antenna. Double dip is observed in the reflection coefficient graph because the four parasitic patches elements are connected to the main patch resulting in strong near-field coupling. In this research, the impact of multi-parasitic elements in gain increment also has been investigated. Firstly, a single parasitic strip is placed adjacent to the radiator. Then, another parasitic strip is added consecutively resulting in four parasitic

34

elements along the main radiator as depicted in Figure 3.12. Note that all parasitic elements shares the same shape and width but vary in length.
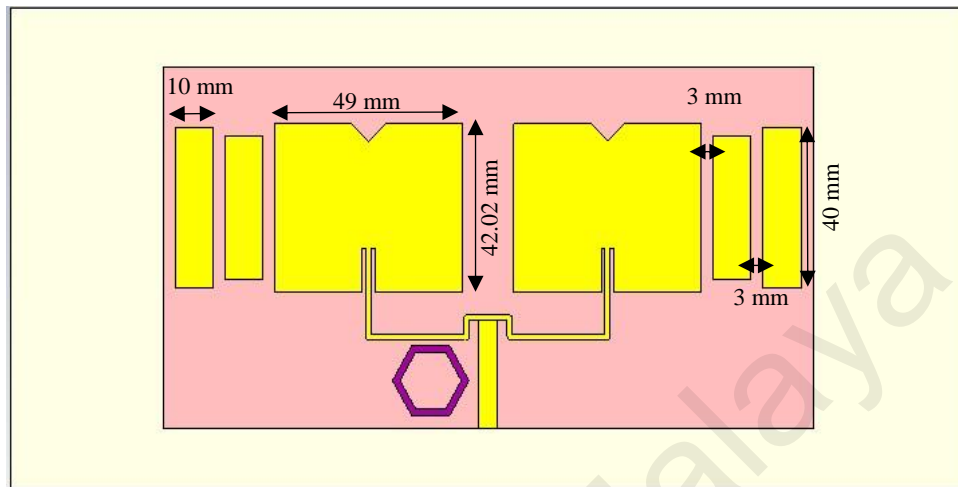
Figure 3.12: Proposed second design of 2x1 array on-body antenna
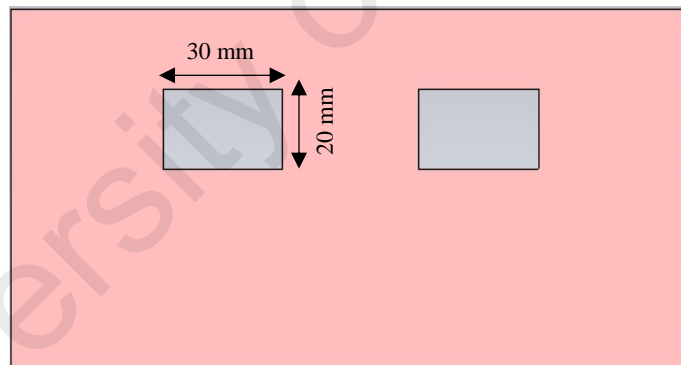
Figure 3.13: Final dimension of slots in substrate for both design

4x1 array on-body antenna is also modified by curving the edge of transmission lines. Furthermore, change is also implemented at the feedline by lengthening its length to 28 mm. This results in alteration of current path as well. Two square slots of 14 mm x 14 mm dimension are also cut from the substrate. The final dimensions of proposed 4x1 array antenna and substrate configuration are shown in Figure 3.14 and Figure 3.15 respectively.
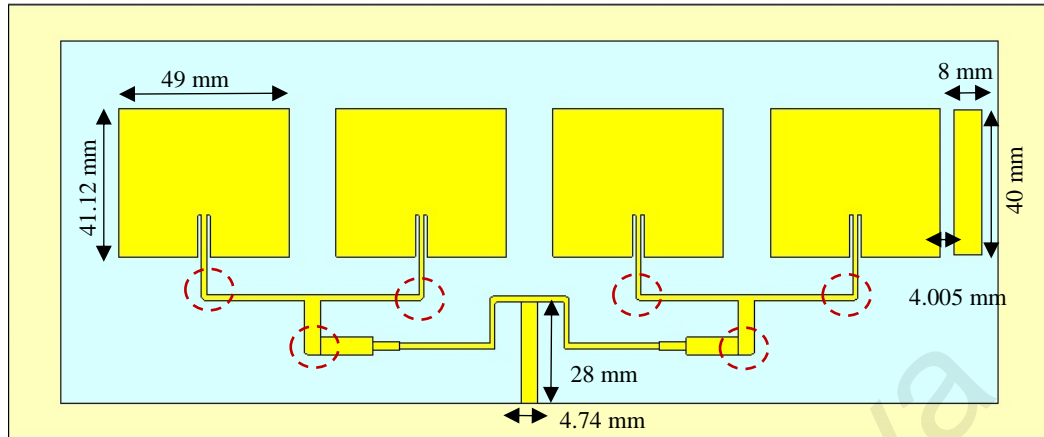
Figure 3.14: Final proposed 4x1 on-body antenna array
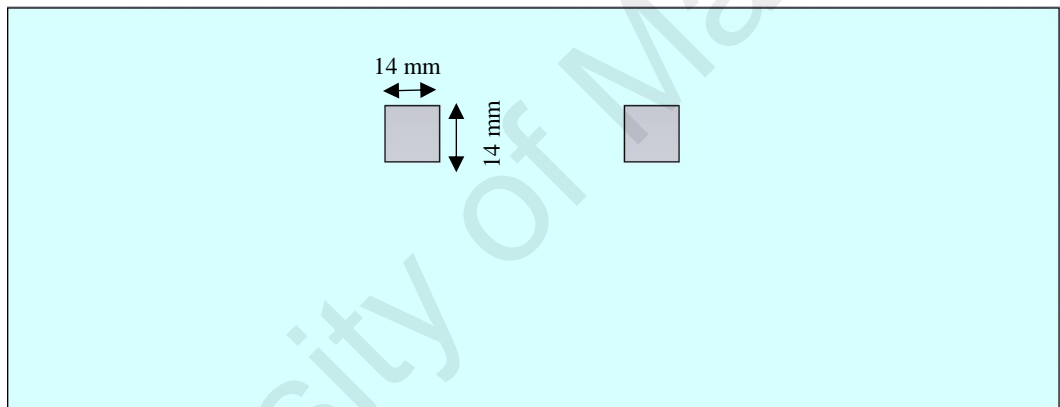
Figure 3.15: Substrate geometry of 4x1 on-body antenna array

CHAPTER 4: RESULTS AND DISCUSSIONS

4.1   Introduction

The evaluation of antenna performance in two scenarios, first one in free space and then onto the human body is presented in this chapter. The characteristics of antennas include reflection coefficient, bandwidth, efficiency, VSWR, radiation pattern, gain and directivity. Parametric analysis of on-body antennas due to variation in tissue thickness are also described here. The last section of this chapter presents several improvement techniques of antenna performance to minimize the antenna-body coupling.

4.2   Antenna Performance in Free Space

4.2.1   Dimensional Analysis of Single Element Patch Antenna

It is crucial to investigate the influence of parameters such as length and width on antenna performance. This can be realized by varying the antenna parameters of patch, feed transmission line and etcetera during the designing stage. The optimization process aids an antenna designer in selecting the best antenna configuration. This section highlights the numerical analysis of parametric study performed on single element patch antenna for RT Duroid 5880 substrate. Reflection coefficient, S_{11} is calculated by varying the inset feed length, notch gap width and patch length and width.

Reflection coefficient, S_{11} represents the ratio of amplitude of reflected voltage wave, V^- to incident voltage wave, V^+ at the load. It describes how much power is returned to the transmitter device. Reflection of power occurs when an antenna is mismatched to the receiver. In order to ensure that an antenna received maximum power, the source impedance

and transmission line must be well coordinated to its characteristic impedance. To design a good antenna, S_{11} of less than -10 dB must be achieved which implies 90 % of the input power is transmitted and the remaining 10 % of the power is reflected.
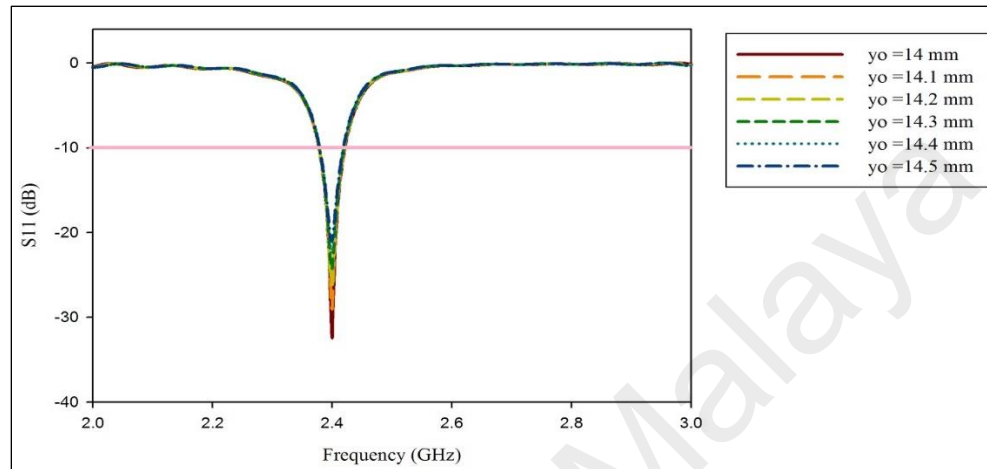
Figure 4.1: Influence of inset feed length, yo on antenna performance
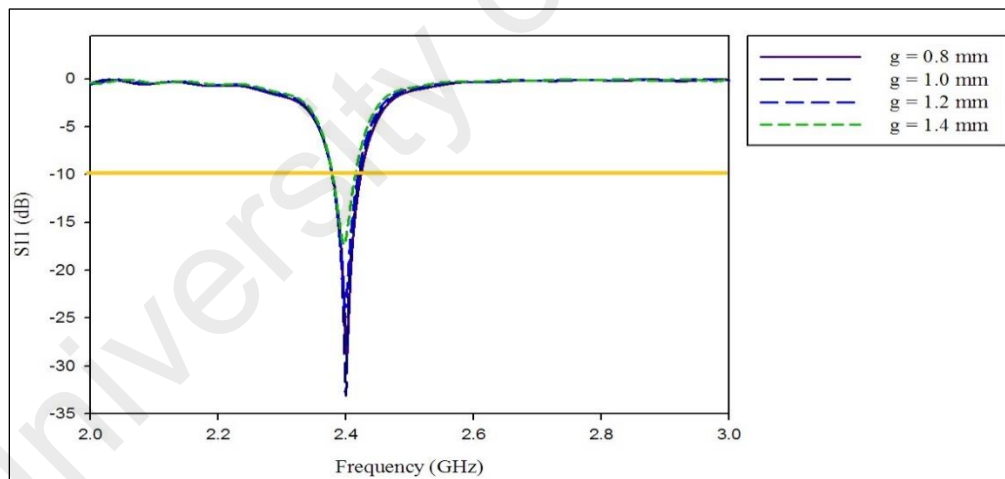
Figure 4.2: Influence of notch gap width, g on antenna performance

Figure 4.1 reveals that there has been only slight variation in reflection coefficient, S_{11} when the length of the inset feed, yo is increased from 14 mm to 14.5 mm with a step size of 0.1 mm. The S_{11} value at 2.4 GHz is -32.247 dB which when yo is 14 mm and -20.988 dB for 2.3988 GHz when yo is tuned to 14.5 mm. It has been mentioned in the previous

chapter that yo is the inset length from the radiating edge. Based on the theory mentioned in [10], varying the location of where the feed line connects to the patch antenna, input impedance can be controlled. Therefore, selection of inset length of 14 mm indicates that the patch impedance is closer to the feed line impedance. Figure 4.3 shows that at 2.4 GHz, the input impedance is almost at the point '1' of the unit circle of the smith chart. This denotes the real part of the impedance is almost 50 Ω which represents good impedance matching.
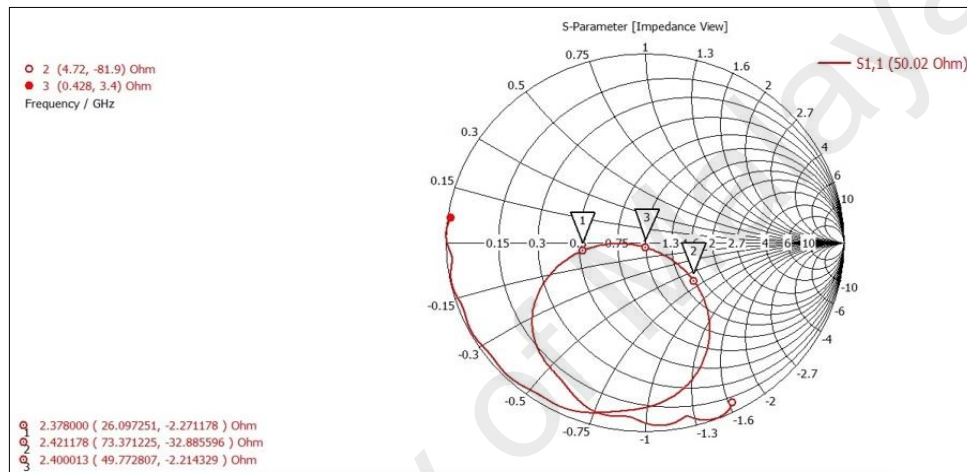
Figure 4.3: Smith chart

Figure 4.2 illustrates the dependency of resonant frequency with notch gap width, g. The operating frequency is deviated slightly with variation in the inset feed width. When g is incremented from 1 mm to 1.4 mm, the frequency shifts from 2.4 GHz to 2.3971 GHz with S_{11} of -17.268 dB. In contrast, the frequency shifts to the right to 2.401 GHz when g is 0.8 mm with S_{11} of -28.991 dB. The best impedance matching can be achieved when the width, g is set at 1 mm where the S_{11} value is -33.044 dB at 2.4 GHz.
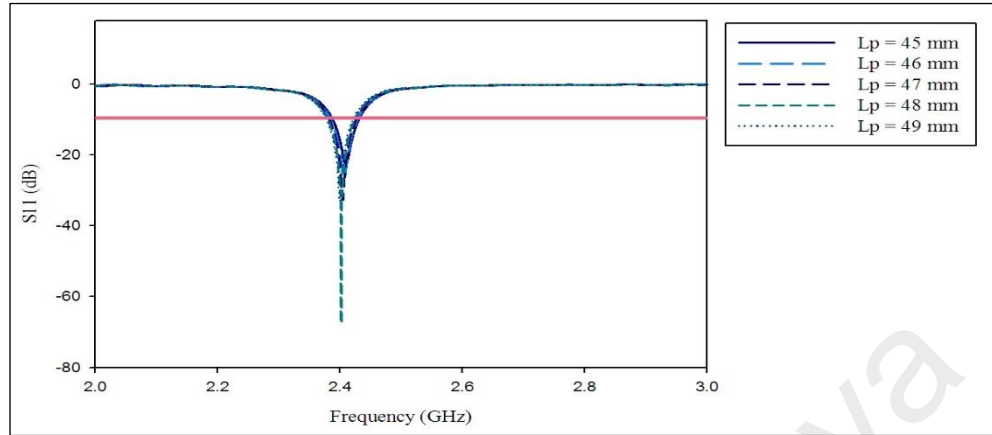
Figure 4.4: Impact of patch length, Lp on antenna performance
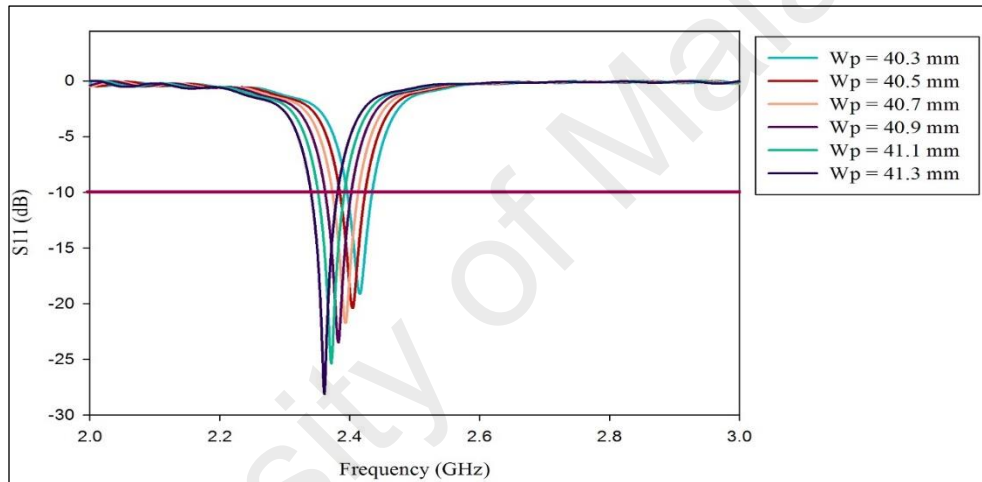
Figure 4.5: Impact of patch width, Wp on antenna performance

The S_{11} graphs in Figure 4.4 and Figure 4.5 represent the impact of varying patch length, Lp and patch width, Wp respectively. A sharp dip is observed when Lp is tuned to 48 mm. It marks a value of -67.402 dB at 2.402 GHz. Besides that, a bandwidth of 43.7 MHz is also achieved for 2.4 GHz ISM band. On the contrary, S_{11} value at 2.4 GHz is -33.044 dB when Lp is increased to 49 mm. A bandwidth of 47.4 MHz is achieved for that particular center frequency which is comparatively higher.

A distinct shift in frequency is observed in Figure 4.5 when the patch width is decreased by -0.2 mm. An accurate explanation for this is that the patch width is inversely proportional to the operating frequency proven by equation 3.1. A S_{11} value of -21.713 dB is obtained at 2.3932 GHz when the width of the patch, Wp is equivalent to 40.7 mm. Further shift is detected when Wp is decreased to 40.5 mm. The S_{11} shifts from its initial position to the left that is 2.4044 GHz. This signifies that performance of an antenna is extremely responsive to the patch width parameter. Thus, it need to be tuned to an optimum value to achieve targeted results.

The final values of dimension which gives best reflection coefficient, S_{11} at required operating frequency are selected and stated in Table 4.1:

Table 4.1: Final dimensions of single element patch antenna

Parameter	Lp	Wp	yo	g
Dimension (mm)	49	40.6	14	1

4.2.2 Performance Analysis of Single Element and Antenna Arrays

The goal of antenna array design is to achieve high gain and directivity which are dependent on number of elements selected based on requirement. The elements can be arranged in many ways on a substrate to form various geometry. Antenna configuration can be classified as linear, planar, and circular and etcetera. The overall radiation pattern of antenna array is shaped by taking number of elements used and spacing between them into consideration. The simulation process is initiated with two elements aligned in linear form with inter-element spacing of 0.4λ, 0.45λ and 0.5λ for FR-4 substrate. The 2x1 antenna array

has a ground dimension of 160 mm x75 mm. The simulation results for 2x1 array antenna are recorded in Table 4.2.

Table 4.2: Influence of IES between elements on antenna performance

IES spacing (d)	fr (GHz)	S_{11} (dB)	BW (MHz)	VSWR	Gain (dB)	Directivity (dB)
0.5 λ	2.394	-53.39	71.5	1.004	6.846	8.982
0.45 λ	2.396	-37.629	74.3	1.003	6.704	8.751
0.4 λ	2.4014	-21.948	66	1.173	6.483	8.481

Table 4.3: Effect of IES between elements on HPBW

	0.4 λ		0.45 λ		0.5 λ	
Element	HPBW	SLL (dB)	HPBW	SLL (dB)	HPBW	SLL (dB)
2	58.1°	-14.8	54.2°	-14.9	50.8°	-15

Radiation pattern in E-plane is more significant for electrical type antennas. The E-plane cut is obtained by varying the theta, θ while keeping phi, φ constant. Thus, the stimulated gains are recorded when phi is equivalent to zero. The highest gain and directivity is recorded when the two elements are spaced apart by 0.5λ. Half Power Beam Width (HPBW) is the coverage angle of an antenna within acceptable half-power limit (-3dB). Additionally, side lobes are beam that are adjacent to main lobe. A diminutive decrease in SLL and a gradual increase in HPBW is noticed when the elements spacing is reduced from 0.5λ to 0.4λ. The spacing between the elements is fixed at 0.5 λ.

Further experiment is conducted by varying the ground plane dimension. Table 4.4 describes the influence of varying ground plane dimension on antenna performance:

Table 4.4: Effect of ground plane dimension on antenna performance

Ground dimension (mm x mm)	fr (GHz)	S_{11} (dB)	BW (MHz)	VSWR	Gain (dB)	Directivity (dB)
160 x 70	2.394	-47.017	74.7	1.008	6.771	8.927
160 x 75	2.394	-53.39	71.5	1.004	6.846	8.982
160 x 80	2.395	-53.397	74	1.004	6.875	9.02
160 x 85	2.395	-44.49	73	1.011	6.905	9.074
165 x 80	2.395	-52.629	73.4	1.005	6.901	9.046

The simulation results verifies that the highest reflection coefficient and good gain for FR-4 substrate can be achieved with ground plane dimension of 160 mm x 80 mm at spacing of 0.5 λ. The effectiveness of array structure in gain improvement of antenna is also investigated by designing 4 x 1 linear array. The comparison in antenna performance for single element and antenna array is listed in Table 4.5. Figure 4.6 and Figure 4.7 show 2D polar plot and 3D far field plot of gain respectively.

Table 4.5: Comparison between single patch and antenna arrays

Number of elements	fr (GHz)	S_{11} (dB)	BW (MHz)	Gain (dB)
Single	2.4	-28.087	60	4.09
2x1	2.395	-53.397	74	6.875
4x1	2.401	-26.45	93.2	9.471

Farfield Gain Abs (Phi=0)

Phi= 0 Phi=180

Theta / Degree vs. dB

Frequency = 2.395
Main lobe magnitude =   6.87 dB
Main lobe direction =   0.0 deg.
Angular width (3 dB) =   50.9 deg.
Side lobe level = -15.1 dB

(a) 2x1 array

Farfield Gain Abs (Phi=0)

Phi= 0 Phi=180

Theta / Degree vs. dB

Frequency = 2.4
Main lobe magnitude =   9.29 dB
Main lobe direction =   1.0 deg.
Angular width (3 dB) =   25.1 deg.
Side lobe level = -11.5 dB

(b) 4x1 array

Farfield Gain Abs (Phi=0)

Phi= 0 Phi=180

Theta / Degree vs. dB

Frequency = 2.4
Main lobe magnitude =   7.54 dB
Main lobe direction =   27.0 deg.
Angular width (3 dB) =   31.9 deg.
Side lobe level = -19.6 dB

(c) 2x2 array

Figure 4.6: Gain 2D polar plot at xz plane for antenna arrays
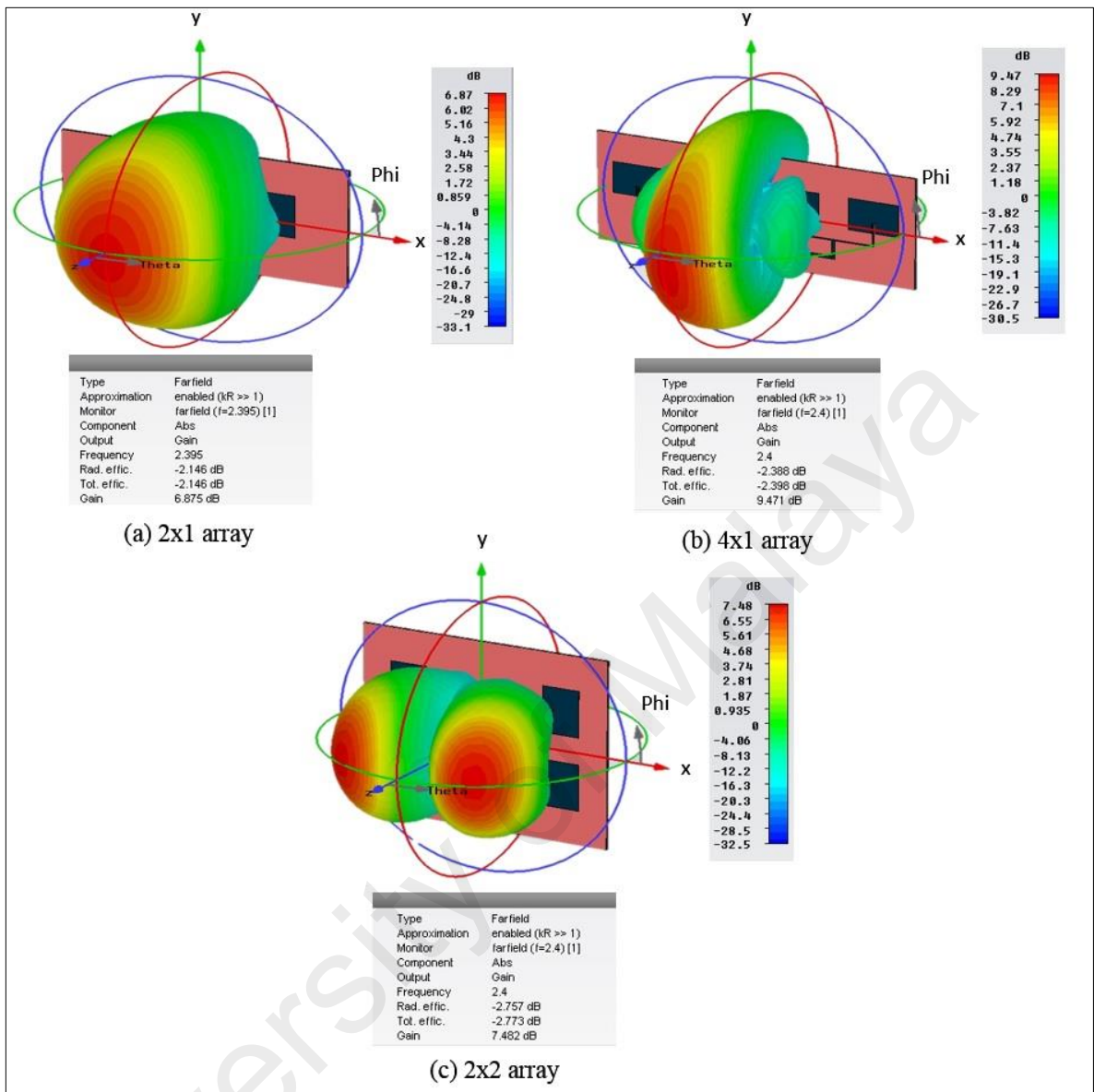
Figure 4.7: Gain 3D far field plot for antenna arrays

The reflection coefficient, S_{11} is the best for 2x1 array configuration which denotes excellent impedance matching. Moreover, it is clearly noticed that bandwidth and gain increases as number of elements increases. The illustrations in Figure 4.6 show narrower main beam width of array antenna is obtained by increasing the number of elements. This further confirms the theory that higher gain or directivity can be achieved with smaller beam

area. The comparison of radiation pattern between 2x1 array and 4x1 array antenna as shown in Figure 4.7 clearly reveals that the radiation gets more intensified at the center of a sphere. In this research, the proposed four elements array antennas are of linear configuration. The rationale behind this selection is that 2x2 array is not a highly directional antenna as it exhibits two major lobes. The signal is directed to 27 degree with HPBW of 31.9 degree as depicted in Figure 4.5 (c). The disadvantage of such arrangement is that the power is not focused at one particular direction only but it is radiated in other direction as well. A high gain of 9.471 dB is achieved with 4x1 compared to 7.482 dB by 2x2 array configuration.

At initial stage, the design and simulation process of antennas were carried out by using FR-4 substrate. In order to select the best configuration for antennas, the comparison were made by replacing the original substrate with RT Duroid 5880 and R0 3730. The simulation results for both materials are described in Table 4.6.

Table 4.6: Performance analysis for different substrate materials

Materials	Number of elements	fr (GHz)	S_{11} (dB)	BW (MHz)	Gain (dB)	Directivity (dB)	η (%)
RT Duroid 5880	Single	2.4	-33.028	48.6	6.667	7.239	92
	2x1	2.401	-23.178	38.9	9.399	9.915	94.7
	4x1	2.4	-15.297	37.6	12.12	12.57	96.4
R0 3730	Single	2.4	-31.697	37.6	6.283	7.119	88.3
	2x1	2.4	-18.13	46.2	8.425	9.114	92.4
	4x1	2.4	-17.845	36.1	11.01	11.8	93.3

4.3   Antenna Performance on the Human Body

The proposed antennas behavior are analyzed in the propinquity of simplified three-layer human body model. The thickness of each body tissue is set at 3 mm. The comparison between characteristics of the antenna in air and on the body is presented in Table 4.7.

46

Table 4.7: Comparison between antenna performance in free space and on-body

Material	Number of elements	Free-space (In air)				On the Human Body				Gain Difference	Gain Difference
		Fr (GHz)	S_{11}(dB)	BW(MHz)	Gain (dB)	Fr (GHz)	S_{11}(dB)	BW(MHz)	Gain (dB)	(dB)	(%)
Rogers RT/ Duroid 5880	Single	2.4	-33.028	43.2	6.667	2.4	-17.161	36.8	7.009	0.342	105.1
	2 x 1	2.401	-23.178	48.6	9.399	2.4	-25.284	53.8	9.23	-0.169	1.8
	4 x 1	2.4	-15.297	38.9	12.12	2.4	-35.173	52.3	11.95	-0.17	1.4
Rogers RO 3730	Single	2.4	-31.697	37.6	6.283	2.4	-22.341	35.9	6.28	-0.003	0.005
	2 x 1	2.4	-18.13	46.2	8.425	2.4	-20.895	47	8.12	-0.305	3.62
	4 x 1	2.4	-17.845	36.1	11.01	2.4	-13.394	33.1	10.84	-0.17	1.54
FR4	Single	2.4	-28.087	60	4.09	2.412	-22.092	50.4	3.37	-0.72	17.6
	2 x 1	2.395	-53.397	74	6.875	2.401	-43.187	70.7	6.452	-0.423	6.15
	4 x 1	2.401	-26.45	93.2	9.471	2.4	-22.87	101.3	8.563	-0.627	6.82

It is noticed that the reflection coefficient, S_{11} is shifted from 2.395 GHz to 2.401 GHz when 2x1 array antenna for FR-4. In addition, the S_{11} is greatly reduced from -53.397 dB to -43.397 dB as the input impedance of antenna detuned from 50.07 Ω to 50.01 Ω. This clearly shows that antenna's reactive field is very sensitive to the vicinity of the body. The existing models of RT Duroid 5880 and R0 3730 on-body antennas are redesigned to meet the requirement of 2.4 GHz ISM band.

It is also can be seen distinctly that radiation pattern and gain of the antennas are affected by the interaction. Antenna gain is naturally reduced due to absorption of power by the body tissues. However, gain increases by 0.342 dB for single element antenna for RT Duroid 5880 as a result of reflections from the body. The comparative study also reveals that RT Duroid 5880 results in low gain loss compared to FR-4 of the same thickness, 1.6 mm. Such performance is attributed by low loss tangent value of 0.0009 compared to 0.0025 for FR-4. Therefore, it can be concluded that RT Duroid 5880 is the best substrate material to design on-body antenna.

4.3.1   Parametric Analysis of Variation in Body Tissue Thickness

The performance of the antenna configurations designed using RT Duroid 5880 are evaluated by placing them on the realistic body tissue. The parametric investigation is carried out by varying the thickness of a body tissue while keeping others constant at chest region. Table 4.8 and Table 4.9 verifies the effect of varying tissue thickness on single element antenna performance.

Table 4.8: Effect of varying skin and muscle thickness on single element antenna performance

Body Tissue Type	Gender	Layer Thickness (mm)	Fr (GHz)	S_{11}(dB)	BW(MHz)	Gain (dB)
Skin	Adult	2	2.4	-17.159	36.5	7.033
		3	2.4	-17.161	36.8	7.009
		4.5	2.4	-16.948	36.2	6.943
Muscle	Adult	20	2.4	-16.64	35.7	6.832

Table 4.9: Effect of varying fat tissue thickness on single element antenna performance

Body tissue type	Gender	BMI Classification	Layer thickness (mm)	Fr (GHz)	S_{11} (dB)	BW (MHz)	Gain (dB)
Fat	Man	Underweight	2	2.4	-17.242	36.7	7.064
		Normal	4	2.4	-17.045	36.6	6.931
		Overweight	10	2.4	-16.428	35.2	6.909
		Obese	18	2.4	-16.76	36	7.353
	Woman	Underweight	3	2.4	-17.161	36.8	7.009
		Normal	9	2.4	-16.41	35.5	6.814
		Overweight	15	2.4	-16.699	35.8	7.259
		Obese	21	2.4	-16.816	36.2	7.383

From the extensive simulation results, it can be observed that the antenna gains are increased when placed onto the human chest. All the various thickness scenarios exhibits gain increment compared to free space setting which is 6.667 dB for single element antenna. There is no correlation between reflection coefficient, S_{11} and tissue thickness as only a slight variation trend for S_{11} and bandwidth is noticed. Besides that, the highest antenna gain is observed for fat tissue thickness of obese man and woman respectively. A rising trend is also revealed when the hypodermis layer thickness is set from 9 mm onwards. Such results show

that reflection effect from the body is very strong as fat layer being less conductive separates

the proximity between two highly conductive skin and muscle tissue.

Table 4.10: Effect of varying skin and muscle thickness on 2x1 array antenna performance

Body Tissue Type	Gender	Layer Thickness (mm)	Fr (GHz)	S_{11}(dB)	BW(MHz)	Gain (dB)
Skin	Adult	2	2.4	-25.388	53.8	9.266
		3	2.4	-25.284	53.8	9.23
		4.5	2.4	-25.098	53.8	9.293
Muscle	Adult	20	2.4	-25.202	53.7	9.346

Table 4.11: Effect of varying fat tissue thickness on 2x1 array antenna performance

Body tissue type	Gender	BMI Classification	Layer thickness (mm)	Fr (GHz)	S_{11} (dB)	BW (MHz)	Gain (dB)
Fat	Man	Underweight	2	2.4	-25.353	53.8	9.283
		Normal	4	2.4	-25.218	53.8	9.207
		Overweight	10	2.4	-25.558	53.8	9.518
		Obese	18	2.4	-26.007	53.8	9.566
	Woman	Underweight	3	2.4	-25.284	53.8	9.23
		Normal	9	2.4	-25.455	53.8	9.5
		Overweight	15	2.4	-25.962	53.8	9.549
		Obese	21	2.4	-25.947	53.8	9.57

As previously stated, the 2x1 array configuration is remodeled to match the input

impedance back to 50 Ω. Only a slight change occurs to the reflection coefficient, S_{11} value

as a consequence of variation in tissue thickness. Additionally, no change occurs to the

bandwidth. Therefore, near field of 2x1 array antenna is less sensitive to the varying nature

of body tissue. However, its radiation property is slightly affected because of deviation in

gain value.

Table 4.12: Effect of varying skin and muscle thickness on 4x1 array antenna performance

Body Tissue Type	Gender	Layer Thickness (mm)	Fr (GHz)	S_{11}(dB)	BW(MHz)	Gain (dB)
Skin	Adult	2	2.4	-35.435	52.3	11.95
		3	2.4	-35.173	52.3	11.95
		4.5	2.4	-34.912	52.3	11.93
Muscle	Adult	20	2.4	-35.081	52.3	11.91

Table 4.13: Effect of varying fat tissue thickness on 4x1 array antenna performance

Body tissue type	Gender	BMI Classification	Layer thickness (mm)	Fr (GHz)	S_{11} (dB)	BW (MHz)	Gain (dB)
Fat	Man	Underweight	2	2.4	-35.135	52.3	11.96
		Normal	4	2.4	-35.175	52.3	11.94
		Overweight	10	2.4	-34.568	52.3	11.89
		Obese	18	2.4	-34.239	52.3	12.02
	Woman	Underweight	3	2.4	-35.173	52.3	11.95
		Normal	9	2.4	-34.679	52.3	11.89
		Overweight	15	2.4	-34.253	52.3	11.97
		Obese	21	2.4	-34.34	52.3	12.06

Similar trend is observed for reflection coefficient, S_{11} and bandwidth of 4x1 array antenna. The antenna still provides $S_{11} <- 10$ dB with bandwidth of 52.3 MHz compared to 38.9 MHz at free space. The gain value slightly decreased by the range from 1.4 % to 1.6 % when the skin thickness increases. The slightest variation in gain is recorded for hypodermis thickness of obese woman which is 0.5 %.

4.3.2   Analysis of Gain Improvement Methods for On-body Antennas

As described in chapter 3, preliminary investigation is carried out by placing the antennas on three-layer tissue of same thickness. The transmission line of the on-body antennas is altered to minimize the attenuation of reflection coefficient, S_{11} and gain. Numerical analysis of the improvement is presented in Table 4.14.

Table 4.14: Impact of modification at transmission line on array antenna performance for RT Duroid 5880

No. of elements	Configuration	Fr (GHz)	S_{11}(dB)	BW(MHz)	Gain (dB)
2 x 1	Original	2.4	-26.776	52.4	9.18
	Curved edge	2.4	-25.284	53.8	9.23
4 x 1	Original	2.4	-19.574	46.7	11.93
	Curved edge	2.4	-35.173	52.3	11.95

Table 4.15 describes the variation in simulated gain when the skin and fat tissue thickness is set for 3 mm respectively and muscle tissue as 20 mm. Antenna performance on the body is further investigated with a 8x1 array configuration for comparison purposes. It is observed that more gain losses are incurred by increasing the complexity of the antenna. These findings raise intriguing questions regarding the usefulness of array structure for body centric communication. The simulated gain with presence of human body is stated in Table 4.15.

Table 4.15: Simulated antenna gain on the body

Number of elements	Gain (dB)			
	Free-space (On air)	On the Human Body	Difference (dB)	Difference (%)
Single	6.667	6.832	0.165	102.5
2x1	9.399	9.346	-0.053	0.56
4x1	12.12	11.91	-0.21	1.73
8x1	15.07	14.32	-0.75	4.98

4.3.2.1 Improvement Results for First Proposed Design of 2x1 Array Antenna

Table 4.16 summarizes the simulated gain obtained through implementation of modification technique for the first proposed antenna structure.

Table 4.16: Gain improvement for the first design of 2x1 array antenna

Modification method	Gain (dB)
Original	9.346
Feed = 22mm	9.434
Parasitic ring (circle)	9.449
Hexagon ring (copper)	9.471
Modified Transmission Line	9.496
Square slot removal (substrate)	9.574
Hexagon ring (aluminium)	9.657

Modification	Gain (dB)
Ground dimension	9.687
Parasitic strip	9.791
Patch slit	9.816
Strip slit	9.911
Extend slot (removal)	9.924
Strip - Octagon slit 1	9.964
Strip - Octagon slit 2	10.02

Alteration done to transmission line structure compared to standard transmission line and the feed length improves the current path resulting in gain enhancement by 0.113 dB. Additional improvement is made with the placement of a circular parasitic ring adjacent to the T-junction which yields a gain increment of 0.015 dB. The logic behind this is that the fringing fields at antenna edges facilitates the emission of microstrip patch antenna. Thus, parasitic elements should be placed near to the radiation edge to produce an electromagnetic coupling. It is observed that hexagon ring made of aluminum provides better gain of 0.083 dB compared to the copper hexagon ring with 0.022 dB.

An improvement is also noticed with removal of square slot from the substrate under the radiator reducing dielectric losses. Two identical parasitic strips are added to the array design which leads to gain enhancement by 0.104 dB. The array structure is further

modified by slit loading in the two patches and the parasitic strips. Figure 4.8 displays the surface current distribution of the array antenna with parasitic elements and slits.
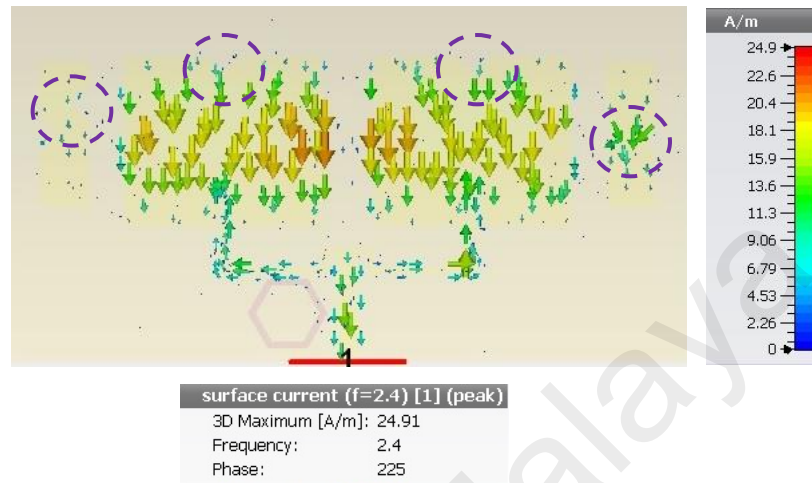
Figure 4.8: Current distribution for the first proposed design

It is clearly noticeable that the current from the radiator is induced into the parasitic strips. In addition, slit creation at the edges of the patch and the parasitic strips disturbs the current flow path leading to gain increment. The current that flows in the same direction is now concentrated at the slit region. The gap between the patches and the parasitic strips have been picked as a parameter to be investigated. Figure 4.9 and Figure 4.10 demonstrate the impact of the spacing on S_{11} and current distribution respectively.
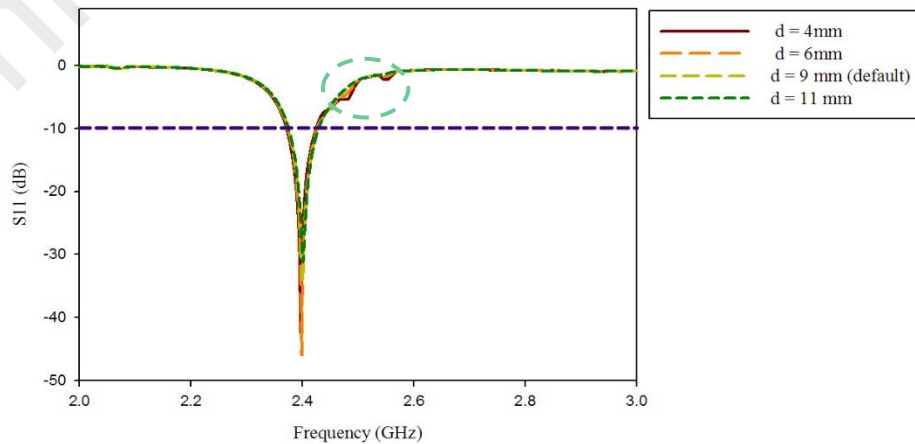
Figure 4.9: Influence of spacing between the radiating elements on S_{11}

(a) d = 4 mm   (b) d = 6 mm

(c) d = 9 mm (default)   (d) d = 11 mm
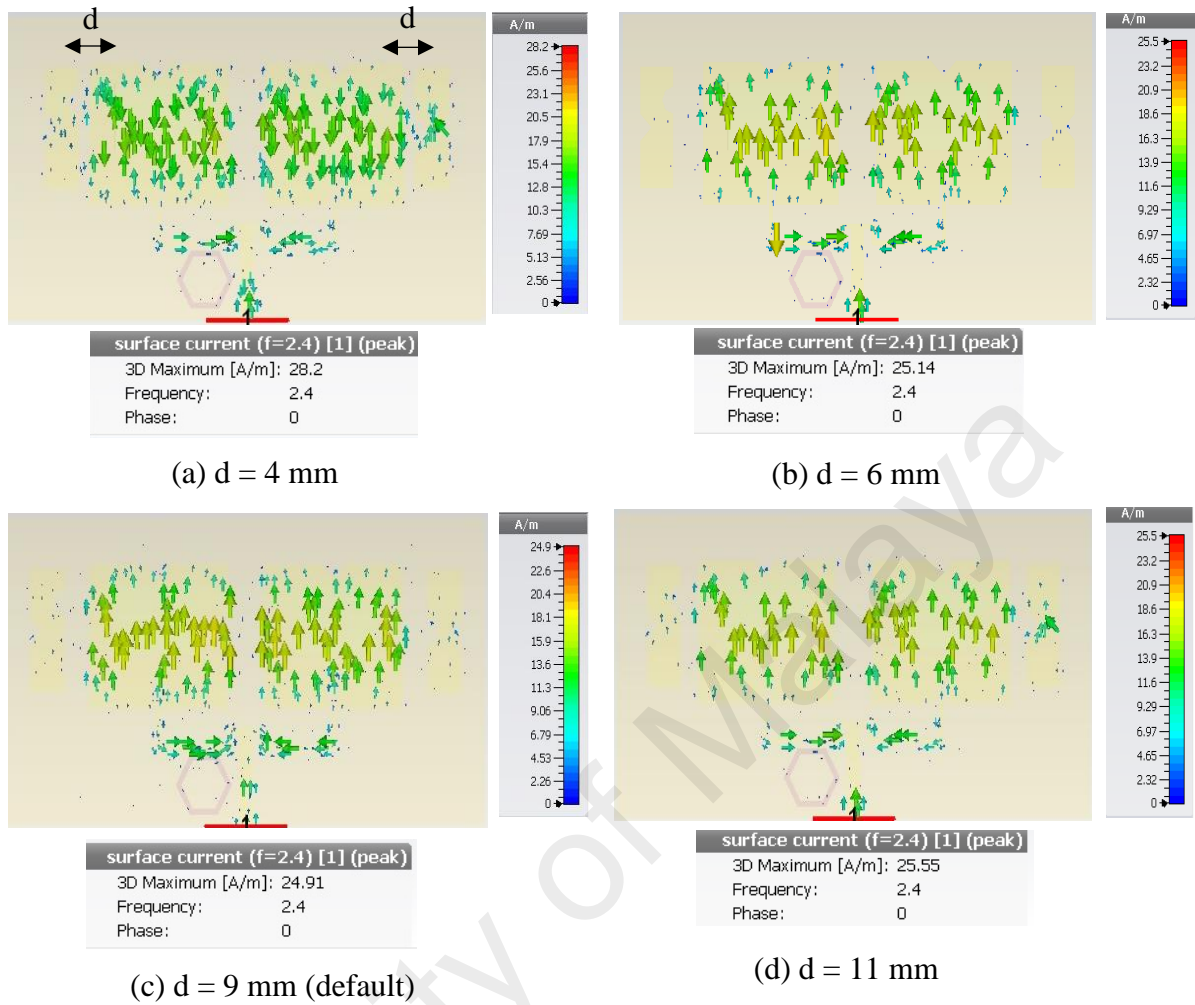
Figure 4.10: Influence of spacing, d on current distribution

The most obvious finding to emerge from the results is that detection of stronger interaction between the elements when the parasitic strip is closely placed with the radiator. The highest current strength is recorded when the spacing is 4 mm while the lowest is for the spacing of 9 mm. As a consequence, the resonant frequency is slightly shifted for both spacing of 4 mm and 6 mm as shown in Figure 4.8. In contrast, no changes is noticed for S_{11} when the parasitic strips are placed farther away but variation in gain is visible. For a spacing of 9 mm, the gain at 2.4 GHz is 10.02 dB whereas 9.916 dB for a spacing of 11 mm.

4.3.2.2   Improvement Results for Second Proposed Design of 2x1 Array Antenna

Gradual increment in gain is noticed when multiple parasitic strips are added to the array design. The gain improvement data are listed in Table 4.17.

Table 4.17: Gain Enhancement for the second design of 2x1 array

No. of parasitic strips	Gain (dB)
Without	9.701
1	9.808
2	9.918
3	9.953
4	10.13

These results further support the idea of gain enhancement with multiple parasitic elements as described in [35] and it is important to mention that no change occurs at the S_{11} graph. Further study is done to analyze the influence of position and dimension of the parasitic elements on antenna's gain. Alignment of the parasitic ring on the right side of the feed line as shown in Figure 4.11 does not influence the gain. However, a change is noticed with the placement of double parasitic ring.

(a) Right

(b) Double
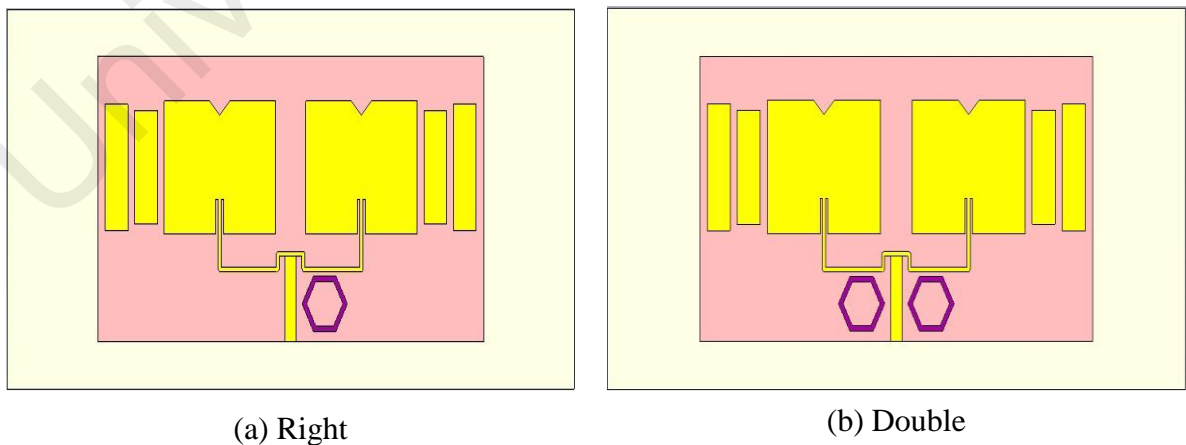
Figure 4.11: Orientation of the parasitic ring

(a) L = 36 mm

(b) L = 38 mm

(c) L = 40 mm

(d) L = 42 mm
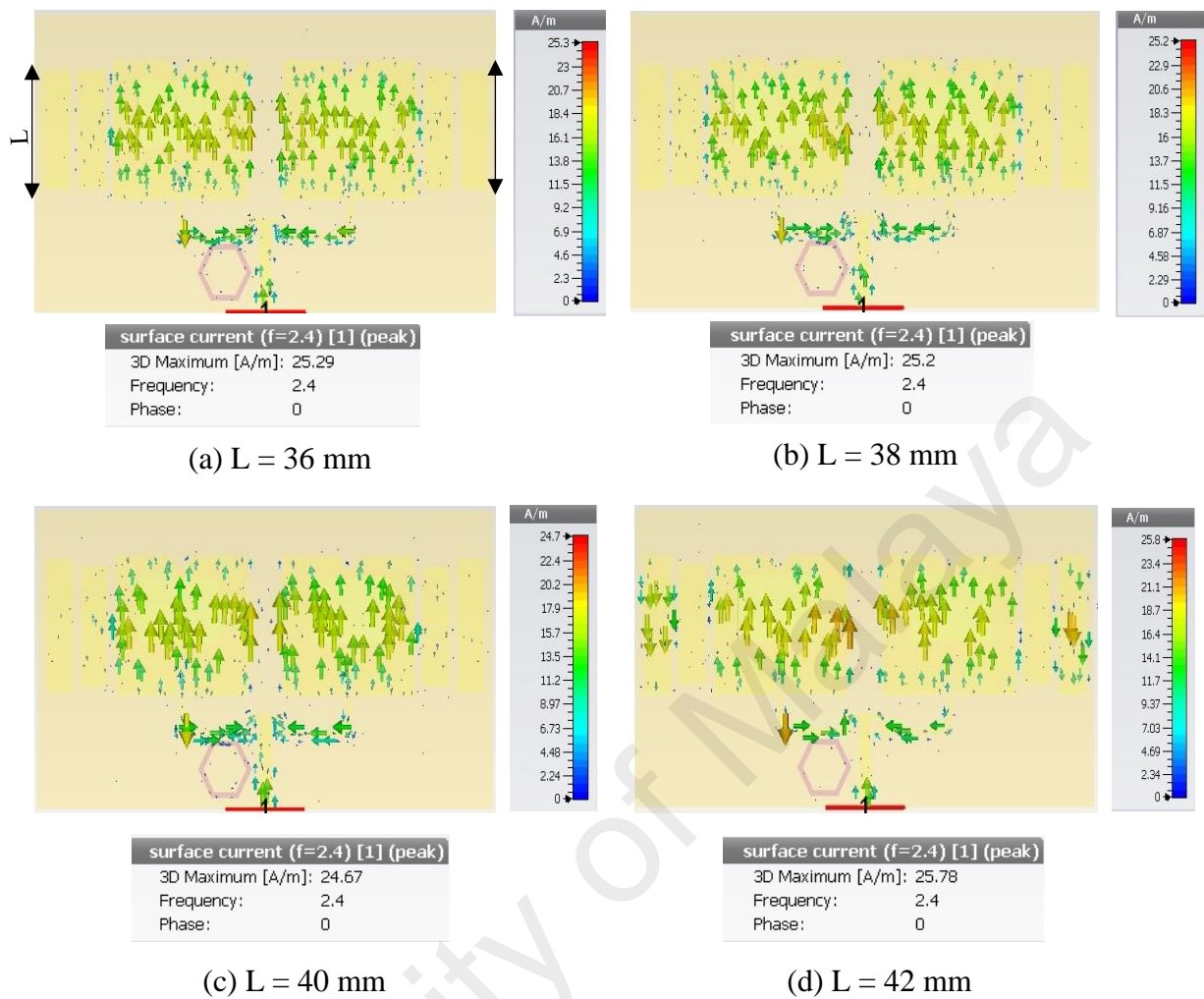
Figure 4.12: Influence of length, L on current distribution

Table 4.18: Influence of length, L on the gain

Length (mm)	S_{11} (dB)	Gain (dB)
36 mm	-33.105	9.943
38 mm	-33.962	10
40 mm	-72.666	10.13
42 mm	-18.03	7.485

A gain value of 10.13 dB is obtained when the hexagon ring is placed on the right side which shows that the parasitic ring can be placed either on the left or right side of the feed. In contrast, double hexagon ring degrades the antenna gain to 10.11 dB. Progressive improvement of gain can be seen when the length of the third and fourth parasitic strip is increased by +2.0 mm. Nevertheless, this could also degrade the antenna performance as the gain is drastically decreased when the strip is lengthened to 42 mm.

### 4.3.2.3   Improvement Results for the Proposed Design of 4x1 Array Antenna

Similar approaches also have been implemented to enhance the 4 elements array antenna performance. Modification of the transmission line has increased the gain by 0.32 dB to 12.23 dB. Next, two square slot is cut from the substrate and a parasitic strip is placed parallel to the fourth patch which contribute to a gain of 12.47 dB. However, significant improvement results are not observed compared to those of 2x1 array antenna. These finding highlights the challenges and complexity of increasing array elements.

4.3.3   Final Performances of the Antenna

In the previous section, several approaches have been addressed and numerically analyzed to overcome the degradation of the performance for both 2x1 and 4x1 array antenna. It is clearly observed that the dimension and position of the parasitic elements are crucially important in enhancing the antenna function. Figure 4.13 represents the comparison of S_{11} of the antenna in free space and on the body while Table 4.19 outlines the overall antenna performance.

58
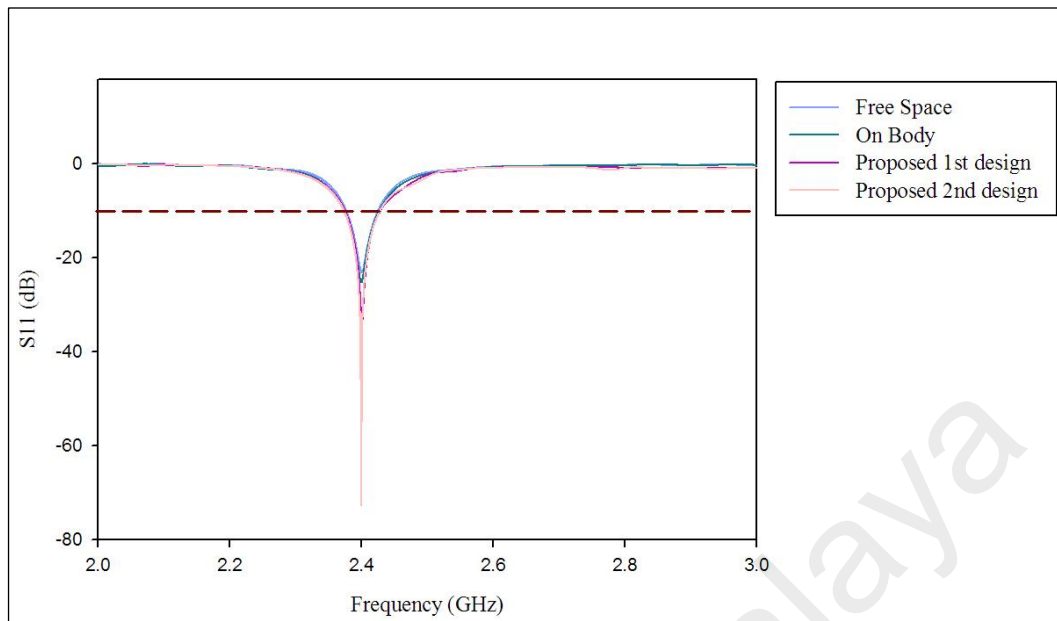
(a) 2 x 1 array antenna
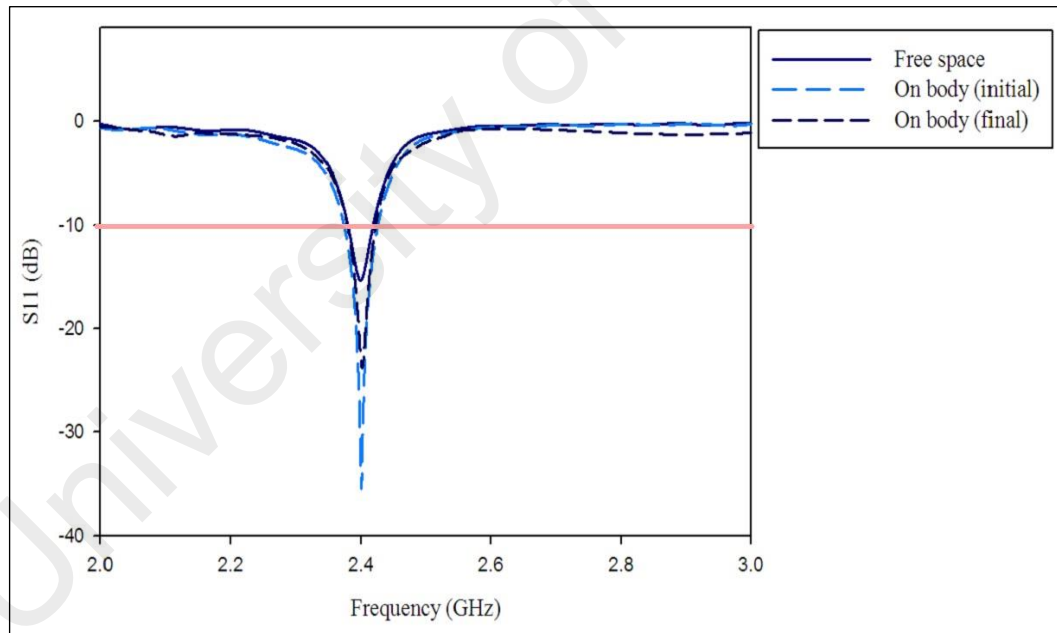
(b) 4 x 1 array antenna

Figure 4.13: Simulated reflection coefficient, S_{11} of the antenna in free space and onto human body

Table 4.19: Simulated overall antenna performance

Number of elements	Antenna Performances	fr (GHz)	S_{11} (dB)	BW (MHz)	Gain (dB)	Directivity (dB)	η (%)
2x1	Free space	2.401	-23.178	38.9	9.399	9.915	94.7
	On-body(initial)	2.4	-25.202	53.7	9.346	10.02	93.3
	On-body(first design)	2.401	-34.511	53.6	10.02	10.36	96.7
	On-body (second design)	2.4	-72.666	55.2	10.13	10.49	96.6
4x1	Free space	2.4	-15.297	37.6	12.12	12.57	96.4
	On-body(initial)	2.4	-35.081	52.3	11.91	12.45	95.7
	On-body(proposed)	2.402	-23.785	43.8	12.47	12.85	97

CHAPTER 5: CONCLUSION

5.1   Summary

The main purpose of this research is to design single element and array antennas that can be located on the body for 2.4 GHz ISM band application. Array antenna provides high gain to overcome attenuation at path loss at longer distance. This is beneficial for body centric communications to stabilize the antenna performance. Since the research only involves simulation process, all the objectives had been achieved, which will be described as follows.

In the beginning stage, all the single and multi-elements antennas are designed using three different substrate material for free-space application. Then, the antennas performance are evaluated for on-body environment. The preliminary results showed that the material with low loss tangent is less sensitive to the human body coupling effect. It is a measure of dissipative energy in that material.

The antenna performance designed using low loss material are then investigated on the actual thickness of the human body in accordance with specific body parts. Such investigations are very important as the human anatomy is unique and proper characterization of on-body antenna is crucial. It is observed that 2x1 array and 4x1 array antenna's near field performance are stable as only slight variation is observed for S_{11} and bandwidth. Besides that, a gradual increase in gain is observed as the thickness of the fat layer of both man and woman increases. However, gain of array antenna decreases with increment in the number of elements when subjected to variation in muscle thickness. This describes the sensitivity of multi-elements configuration to a highly conductive muscle tissue.

The last stage involves reducing the impact of the human body with simple gain enhancement techniques for 2x1 and 4x1 array antenna. The results revealed that the 2x1 array on-body antenna gain is increased by 7.2 % for the first design and 8.4 % for the second proposed design. However, it is only managed to increase the antenna gain by 4.7 % for the 4x1 array on-body antenna. This highlights the complexity of increasing array elements for low frequency applications. However, this scenario will be different for millimeter wave frequencies as array configurations are required to overcome high attenuation losses.

5.2   Future Work

Fabrication and measurement process need to be carried out to validate the performance of the antenna by simulation. Besides that, further study of the material selection is important to improvise the antenna performance on the body. Recent advancement in material engineering introduce materials such as textiles and silicon based polymers such as PDMS, which can be used to develop the flexible antenna design. However, the dielectric constant and conductivity of the materials need to be measured as they are not easily documented.

In this research, the performance of the antenna is evaluated at chest region of a human body. However, it is also important to study the interaction of radio wave at different body parts to encourage suitable antenna design according to application and impact to the user's health.

Lastly, Specific Absorption Rate (SAR) need to be determined by simulation and measurement for the on-body antennas. The electromagnetic absorption by the body tissues should not exceed the threshold level set by IEEE or ICNIRP guidelines. However, accurate density value of the body tissues need to be known in order to evaluate the SAR.

62

REFERENCES

1. Peter S.Hall, Y. H. (2012). Antennas and Propagation for Body-Centric Wireless Communications.

2. Islam, N. A., et al. (2015). Design and performance measurement of an in-body implantable miniaturized Slot Dipole rectangular patch antenna for biomedical applications. 2015 International Conference on Advances in Electrical Engineering (ICAEE).

3. Khaoula Tayari, H. W., Mondher Chaoui, Hamadi Ghariani, Mongi Lahiani (2016). Study of the effects of human tissue on performance of a loop antenna. IOSR Journal of Electrical and Electronics Engineering (IOSR-JEEE).11(4), 6 - 12.

4. Challa, N. R. and S. Raghavan (2015). Design of multiband implantable loop antenna for in body applications. 2015 Conference on Power, Control, Communication and Computational Technologies for Sustainable Growth (PCCCTSG).

5. Psenakova, Z., et al. (2016). Simulation and assessment of pacemaker RF exposure (2.4 GHz) by PIFA antenna. 2016 ELEKTRO.

6. Soontornpipit, P. (2016).Design of Implanted PIFA for Implantable Biotelemetry Locations: Chest and Abdomen. Procedia Computer Science 86: 236-239.

7. Yeboah-Akowuah, B., et al. (2015). A low profile microstrip patch antenna for body-centric communications at 2.45GHz band. 2015 9th European Conference on Antennas and Propagation (EuCAP).

8. Navdeep Kaur, R. (2013). Design and Simulation of Microstrip Patch Antenna for On-Body Communication using Different Feeding Techniques. Proceedings of the Second International Conference on Advances in Electronics, Electrical and Computer Engineering (EEC 2013).

9. Al-Shaheen, A. (2012). New Patch Antenna for ISM Band at 2.45 GHz. ARPN Journal of Engineering and Applied Sciences 7(1), 1-9.

10. Constantine A. Balanis, *Antenna theory third edition analysis and designing*, 3rd Edition, Willey Interscience

11. Cotton, S. L., R. D'Errico, and C. Oestges (2014),A review of radio channel models for body centric communications, Radio Sci., 49, 371 −388, doi:10.1002/ 2013RS005319.

12. L.Nithyanandan, M. A. a. (2014). Analysis of Microstrip Line Feed Triangular Patch Antenna for WLAN (2.4 GHz). Proceedings of International Conference on Advances in Communication, Network, and Computing, CNC.

13. Milligan, T. A. (2005). *Modern Antenna Design*, 2nd Edition, Willey Interscience

14. Melia, G. C. R., et al. (2011). Development of a layered broadband model of biological materials for aerospace applications. 10th International Symposium on Electromagnetic Compatibility.

15. J. Gordon Betts., et al. (2013). *Anatomy and Physiology*. Rice University, OpenStax College.

16. Vladimír, H. (2013). Planar antenna in proximity of human body models. 2013 7th European Conference on Antennas and Propagation (EuCAP).

17. Teruo Onishi., et. al. RF dosimetry using Japanese Anatomical Models.

18. Hossain, T., et al. (2015). Design and performance analysis of a biomedical implantable patch antenna. 2015 International Conference on Advances in Electrical Engineering (ICAEE).

19. Soontornpipit, P. (2014). Design of an Implantable Antenna Feasibility Study for Continuous Glucose Monitoring. ECTI Transactions on Electrical Engineering, Electronics, and Communications 12(1), 44-52.

20. Bouazizi, A., et al. (2016). Parametric study of implantable planar inverted-F antenna for wireless body area network application. 2016 2nd International Conference on Advanced Technologies for Signal and Image Processing (ATSIP).

21. J. Gemio, J. P. o., and J. Soler (2010).Human Body Effects on Implantable Antennas for ISM Bands Applications: Models Comparison and Propagation Losses Study. Progress In Electromagnetics Research, 110,437-452.

22. Christ, A., et al. (2006). The dependence of electromagnetic far-field absorption on body tissue composition in the frequency range from 300 MHz to 6 GHz. IEEE Transactions on Microwave Theory and Techniques 54(5), 2188-2195.

23. Sipal, V., et al. (2013). Evaluation of antenna suitability for the use in radiomyography. 2013 Loughborough Antennas & Propagation Conference (LAPC).

24. Aguilar, S. M., et al. (2011). Design of a microwave breast imaging array composed of dual-band miniaturized antennas. 2011 URSI General Assembly and Scientific Symposium.

25. M. Teja, K. R. D. (2016). Design of Compact Dual Band Slot Antenna at MICS and ISM for Bio-Medical Applications. International Journal of Innovative Research in Computer and Communication Engineering 4(8), 15362 - 15368.

26. Vidal, N. and J. M. López-Villegas (2010). Changes in Electromagnetic Field Absorption in the Presence of Subcutaneous Implanted Devices: Minimizing Increases in Absorption. IEEE Transactions on Electromagnetic Compatibility 52(3), 545-555.

27. Fazeli, M., et al. (2016). Implantable ferrite antenna for biomedical applications. Microwave and Optical Technology Letters 58(11), 2745-2749.

28. Robin Augustine. Electromagnetic modelling of human tissues and its application on the interaction between antenna and human body in the BAN context. Universit´e Paris-Est, 2009.

29. P. Hasgall, F. Di Gennaro, C. Baumgartner, E. Neufeld, M. Gosselin, A. Payne, D. Klingenbck, and N. Kuster, "Itis database for thermal and electromagnetic parameters of biological tissues, v3.0," 2015. [Online].
Available: http://dx.doi.org/10.13099/VIP21000-03-0

30. D. Andreuccetti, R.Fossi and C.Petrucci, "Calculation of the dielectric properties of body tissues in the frequency range 10 Hz – 100 GHz," [Online].
Available at http://niremf.ifac.cnr.it/tissprop/

31. S. Holcombe and S.Wang (2014), Subcutaneous fat distribution in the human torso, pp. 389-396

32. Mohammed Younssi, A. J., Yacoub Diallo, Ahmed El Moussaoui, and Noura Aknin (2013). Study of a Microstrip Antenna with and Without Superstrate for Terahertz Frequency. International journal of Innovation and Applied Studies 3(4), 369-371.

33. Khan, H. A., et al. (2016). Patch antenna using EBG structure for ISM band wearable applications. 2016 International Conference on Intelligent Systems Engineering (ICISE).

34. Alamri, S., et al. (2016). Gain enhancement of implanted antenna using lens and parasitic ring. Electronics Letters 52(10), 800-801.

35. Kaul, N., et al. (2015). Effect of parasitic patch configurations on multi-banding of microstrip antenna. 2015 4th International Conference on Reliability, Infocom Technologies and Optimization (ICRITO)

APPENDICES

RT/duroid® 5870 /5880
High Frequency Laminates

RT/duroid® 5870 and 5880 glass microfiber reinforced PTFE composites are designed for exacting stripline and microstrip circuit applications.

The randomly oriented microfibers result in exceptional dielectric constant uniformity.

The dielectric constant of RT/duroid 5870 and 5880 laminates is uniform from panel to panel and is constant over a wide frequency range.
Its low dissipation factor extends the usefulness of RT/duroid 5870 and 5880 laminates to Ku-band and above.

RT/duroid 5870 and 5880 laminates are easily cut, sheared and machined to shape. They are resistant to all solvents and reagents, hot or cold, normally used in etching printed circuits or in plating edges and holes.

Normally supplied as a laminate with electrodeposited copper of ½ to 2 ounces/ft.² (8 to 70μm) or reverse treated EDC on both sides, RT/duroid 5870 and 5880 composites can also be clad with rolled copper foil for more critical electrical applications. Cladding with aluminum, copper or brass plate may also be specified.

When ordering RT/duroid 5870 and 5880 laminates, it is important to specify dielectric thickness, tolerance, rolled, electrodeposited or reverse treated copper foil, and weight of copper foil required.
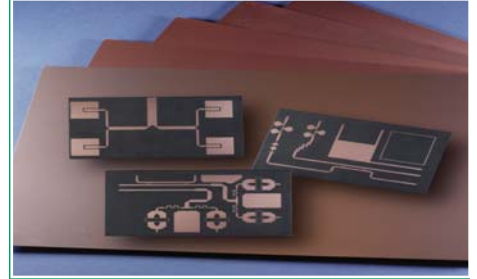
Features:

- Lowest electrical loss for reinforced PTFE material
- Low moisture absorption
- Isotropic
- Uniform electrical properties over frequency
- Excellent chemical resistance

Some Typical Applications:

- Commercial Airline Broadband Antennas
- Microstrip and Stripline Circuits
- Millimeter Wave Applications
- Military Radar Systems
- Missile Guidance Systems
- Point to Point Digital Radio Antennas

Advanced Connectivity Solutions
100 S. Roosevelt Avenue, Chandler, AZ 85226
Tel: 480-961-1382 Fax: 480-961-4533 www.rogerscorp.com

PROPERTY	TYPICAL VALUES			DIRECTION	UNITS[3]	CONDITION	TEST METHOD
	RT/duroid 5870		RT/duroid 5880				
[1]Dielectric Constant, ε_r Process	2.33 2.33 ± 0.02 spec.		2.20 2.20 ± 0.02 spec.	Z Z	N/A	C24/23/50 C24/23/50	1 MHz IPC-TM-650 2.5.5.3 10 GHz IPC-TM 2.5.5.5
[4]Dielectric Constant, ε_r Design	2.33		2.20	Z	N/A	8 GHz - 40 GHz	Differential Phase Length Method
Dissipation Factor, tan δ	0.0005 0.0012		0.0004 0.0009	Z Z	N/A	C24/23/50 C24/23/50	1 MHz IPC-TM-650, 2.5.5.3 10 GHz IPC-TM-2.5.5.5
Thermal Coefficient of ε_r	-115		-125	Z	ppm/°C	-50 - 150°C	IPC-TM-650, 2.5.5.5
Volume Resistivity	2 X 10^7		2 X 10^7	Z	Mohm cm	C96/35/90	ASTM D257
Surface Resistivity	2 X 10^7		3 X 10^7	Z	Mohm	C/96/35/90	ASTM D257
Specific Heat	0.96 (0.23)		0.96 (0.23)	N/A	J/g/K (cal/g/C)	N/A	Calculated

	Test at 23 °C	Test at 100 °C	Test at 23 °C	Test at 100 °C	DIRECTION	UNITS[3]	CONDITION	TEST METHOD
Tensile Modulus	1300 (189)	490 (71)	1070 (156)	450 (65)	X	MPa (kpsi)	A	ASTM D638
	1280 (185)	430 (63)	860 (125)	380 (55)	Y			
ultimate stress	50 (7.3)	34 (4.8)	29 (4.2)	20 (2.9)	X			
	42 (6.1)	34 (4.8)	27 (3.9)	18 (2.6)	Y			
ultimate strain	9.8	8.7	6.0	7.2	X	%		
	9.8	8.6	4.9	5.8	Y			
Compressive Modulus	1210 (176)	680 (99)	710 (103)	500 (73)	X	MPa (kpsi)	A	ASTM D695
	1360 (198)	860 (125)	710 (103)	500 (73)	Y			
	803 (120)	520 (76)	940 (136)	670 (97)	Z			
ultimate stress	30 (4.4)	23 (3.4)	27 (3.9)	22 (3.2)	X			
	37 (5.3)	25 (3.7)	29 (5.3)	21 (3.1)	Y			
	54 (7.8)	37 (5.3)	52 (7.5)	43 (6.3)	Z			
ultimate strain	4.0	4.3	8.5	8.4	X	%		
	3.3	3.3	7.7	7.8	Y			
	8.7	8.5	12.5	17.6	Z			

PROPERTY	TYPICAL VALUES			DIRECTION	UNITS[3]	CONDITION	TEST METHOD
Moisture Absorption	0.02		0.02	N/A	%	.062" (1.6mm) D48/50	ASTM D570
Thermal Conductivity	0.22		0.20	Z	W/m/K	80°C	ASTM C518
Coefficient of Thermal Expansion	22 28 173		31 48 237	X Y Z	ppm/°C	0-100°C	IPC-TM-650, 2.4.41
Td	500		500	N/A	°C TGA	N/A	ASTM D3850
Density	2.2		2.2	N/A	gm/cm^3	N/A	ASTM D792
Copper Peel	27.2 (4.8)		31.2 (5.5)	N/A	pli (N/mm)	1 oz (35mm) EDC foil after solder float	IPC-TM-650 2.4.8
Flammability	V-0		V-0	N/A	N/A	N/A	UL94
Lead-Free Process Compatible	Yes		Yes	N/A	N/A	N/A	N/A

[1] Specification values are measured per IPC-TM-650, method 2.5.5.5 @ ~10GHz, 23°C. Testing based on 1 oz. electrodeposited copper foil. e$_r$ values and tolerance reported by IPC-TM-650 method 2.5.5.5 are the basis for quality acceptance, but for some products these values may be incorrect for design purposes, especially microstrip designs. We recommend that prototype boards for new designs be verified for desired electrical performance.
[2] Typical values should not be used for specification limits, except where noted.
[3] SI unit given first with other frequently used units in parentheses.
[4] The design Dk is an average number from several different tested lots of material and on the most common thickness/s. If more detailed information is required, please contact Rogers Corporation. Refer to Rogers' technical paper "Dielectric Properties of High Frequency Materials" available at http://www.rogerscorp.com.

Standard Thickness	Standard Panel Size	Standard Copper Cladding	Non-Standard Copper Cladding
0.005" (0.127mm) 0.031" (0.787mm) 0.010" (0.254mm) 0.062" (1.575mm) 0.015" (0.381mm) 0.125" (3.175mm) 0.020" (0.508mm) Non-standard thicknesses are available	18" X 12" (457 X 305mm) 18" X 24" (457 X 610mm) Non-standard sizes are available up to 18" X 48" (457 X 1219 mm)	½ oz. (18µm) and 1 oz. (35µm) electrodeposited and rolled copper foil	¼ oz. (9 µm) electrodeposited copper foil ½ oz. (18µm), 1 oz. (35µm) and 2 oz. (70µm) reverse treat copper foil 2 oz. (70µm) electrodeposited and rolled copper foil
		Thick metal claddings may be available based on dielectric and plate thickness. Contact customer service for more information on available non-standard and custom thicknesses, claddings and panel sizes	

RO3730™
Antenna Grade Laminates

RO3730™ laminates have the excellent thermo-mechanical properties and electrical characteristics that antenna designers need. The laminates have a dielectric constant (Dk) of 3.0 and a loss tangent (Df) of 0.0013 measured at 2.5 GHz. These values allow antenna designers to realize substantial gain values while minimizing signal loss. Materials are available with a demonstrated low PIM performance, with values better than -154 dBc (measured using Rogers' internal test method).

RO3730 materials can be fabricated into printed circuit boards using standard PTFE circuit board processing techniques as described in the application note, "Fabrication Guidelines for RO3730 High Frequency Circuit Materials."

Cladding is 1 ounce rolled annealed copper (35 µm thick). RO3730 laminates are manufactured under an ISO 9002 certified quality system.

FEATURES AND BENEFITS

RO3730 reinforced woven fiber glass with optimized glass and filler loading.
- Improved mechanical rigidity
- Easier handling and processing versus non-reinforced PTFE products
- Lower Dissipation factor

Low PIM
- Reduced signal interference

Low Loss
- Improved antenna gain

Economically priced
- Volume manufacturing
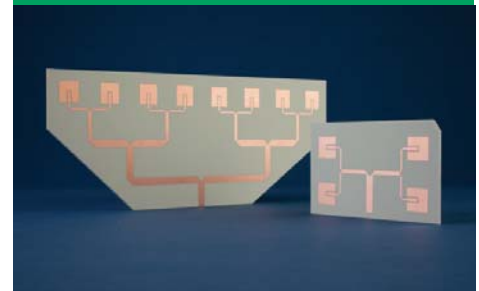
Environmentally friendly
- Lead-free process compatible
- RoHS compliant

Regional finished goods inventories
- Short lead-time / quick inventory turn.
- Efficient supply

SOME TYPICAL APPLICATIONS:

- Base Station Antennas
- RFID Antennas
- WLAN Antennas
- Satellite Radio Antennas

The world runs better with Rogers.®

Property	[1]Typical Value	Direction	Units	Condition	Test Method
Dielectric Constant, ε_r Process	3.00 ± 0.06	Z		10 GHz/23°C	IPC-TM-2.5.5.5
[2]Dielectric Constant, ε_r Design	2.93	Z		8 GHz - 40 GHz	Differential Phase Length Method
Dissipation Factor, δ	0.0016 0.0013	Z		10 GHz/23°C 2.5GHz/23°C	IPC-TM-650, 2.5.5.5
Volume Resistivity	10^7		MΩ•cm	COND A	IPC-TM-650, 2.5.17.1
Surface Resistivity	10^7		MΩ	COND A	IPC-TM-650, 2.5.17.1
Flexural Strength	9 (1.3) 8 (1.2)	X Y	MPa (kpsi)		IPC-TM-650, 2.4.4
Dimensional Stability	0.02 0.03	X Y	mm/m (mils/inch)		IPC-TM-650, 2.4.39A
Coefficient of Thermal Expansion	11	X	ppm/°C		IPC-TM-650, 2.1.41
	12	Y			
	65	Z			
PIM	<-154		dBc		
Td	500		°C		ASTM D3850
Thermal Coefficient of ε_r - TcDK	-22		ppm/°C	-50°C to +150°C	
Thermal Conductivity	0.45		W/m/°K	D24/23	IPC-TM-650 2.6.2.1
Moisture Absorption	0.04		%	D48/50	ASTM D570
Specific Gravity	2.1		gm/cm³	23°C	ASTM D792
Copper Peel Strength	1.8 (10.5)		N/mm (pli)	10 sec. 550°F Solder Float	IPC-TM-650 2.4.8
Flammability	V-0				UL94
Lead-Free Process Compatible	YES				

NOTES:
[1] Typical values are a representation of an average value for the population of the property. For specification values contact Rogers Corporation.
[2] The design Dk is an average number from several different tested lots of material and on the most common thickness/s. If more detailed information is required please contact Rogers Corporation or refer to Rogers' technical reports on the Rogers Technology Support Hub at http://www.rogerscorp.com/acm/technology.

Standard Thickness	Standard Panel Size	Standard Copper Cladding
0.030" (0.762mm) 0.060" (1.524mm)	24"X18" (610mm X 457mm) 24"X54" (610mm X 1.37m)	Rolled Copper Foil: 1 oz. (1RD/1RD)

For more information about RO3000 Series High Frequency Laminates, scan the QR code below